21.May.2005
T. Kobayashi

ATLAS検出器と物理入門(その5)
「アトラス検出器のまとめ」(‥にかえて)

***** M1向けの話 *****

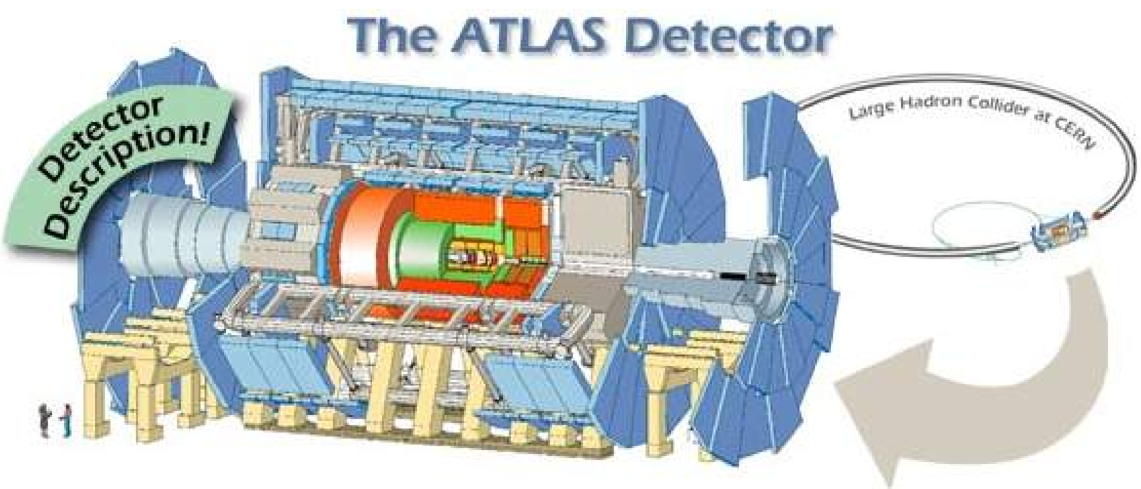

1)そもそもの設計思想は？
目指す物理は？ → ATLAS LoI (1992)

2)実際のchoiceと期待されるperformance → ATLAS Physics TDR (1999)

3)アトラス検出器のkey point(いくつかの例)
- H → llll, $\gamma\gamma$, $\tau\tau$(VBF)
- SUSY (SUGRA, GMSB, ‥)

今日の話の結論

アトラス検出器の性能をよく知り、その特徴を活かした解析を目指してください。

Physics Goals of ATLAS

(as of 1992, LoI)

- sensitivity to the largest possible Higgs mass range
- detailed studies of top quark mass and decays
- Standard Model studies (gauge boson couplings)
- SUSY searches
- sensitivity to large compositeness scales
- search for unexpected new physics

当時は、top未発見, m_H < 1TeV, SUSY or DSB(techni-color), gauge unification(*), SUGRA

(*) Ugo Amaldi, Wim de Boer, Fuerstenau (1991)

その後、top発見、Higgs mass range, GMSB, VBF(**), ED, little Higgs, ・・

(**) Rainwater, Zeppenfeld, 萩原 (1998)

Examples of physics signatures

Higgs searches:

$H \rightarrow \gamma\gamma$ from $pp \rightarrow H+X$ or ttH, WH, ZH with e or μ tags

$H \rightarrow ZZ^* \rightarrow eeee$ or $ee\mu\mu$ or $\mu\mu\mu\mu$

$H \rightarrow ZZ \rightarrow$ as above, $ll\nu\nu$, ll jet+jet ($l=e,\mu$)

$H \rightarrow WW \rightarrow l^+\nu l^-\nu$ or $l\nu$ jet+jet with forward jet tag

$A \rightarrow \tau\tau$

$H^\pm \rightarrow \tau\nu$

Top quark physics:

$tt \rightarrow WbWb \rightarrow l\nu$ + jets plus b–tag

$tt \rightarrow H^\pm bWb \rightarrow \tau\nu + l\nu$ plus b–tag

Supersymmetry:

Main signatures for squark and gluinos are missing E_T plus jet topologies (direct decays) plus W or Z (cascade decays)

Compositeness:

Deviations in the jet cross section from the QCD expectation for very high p_T jets

→ Sensitivity to a variety of final state signatures is needed

Detector goals

Primary goal:

Balanced approach to electron, gamma, muon, jet and missing transverse energy measurements at high luminosity

Additional goals:

During initial lower luminosity, and to as high a luminosity as practicable, more complex signatures including tau detection and heavy flavour tags

- Large acceptance in rapidity and transverse momentum thresholds
- Homogeneous detector layout with only the essential components
- Design within realistic cost constraints

→ Detector performance goal (see Table)

Global detector concept

Powerful inner detector in a 2T central solenoid for accurate momentum measurement of isolated leptons over a large rapidity span ($-2.5 < \eta < 2.5$) and electron identification

High quality EM sampling calorimetry combined with fine granularity preshower detection for electron and gamma detection

Hermetic hadron calorimetry for jet and missing transverse energy measurements ($-5 < \eta < 5$)

Air-core toroid muon spectrometer with large acceptance ($-3 < \eta < 3$) and stand-alone momentum measurement capability

High precision vertex detector for (initial) lower luminosity operation

Modular and flexible trigger, DAQ and analysis architecture

Detector component choice

Inner detector

precision tracking:
- silicon micro strip and pixel detectors

electron identification and continuous tracking:
- straw tube with transition radiation detection (TRT)

Calorimetry

electromagnetic with Pb absorber:
- liquid Argon accordion

hadronic with Fe absorber:
- scintillator tiles and liquid Argon(with Cu)

very forward calorimetry ($3 < |\eta| < 5$):
- liquid Argon in tube/rod with Cu/W

Muon measurements

momentum measurements:
- MDT and CSC

triggering and 2-nd coordinate measurements:
- RPC and TGC

ATLAS Detector

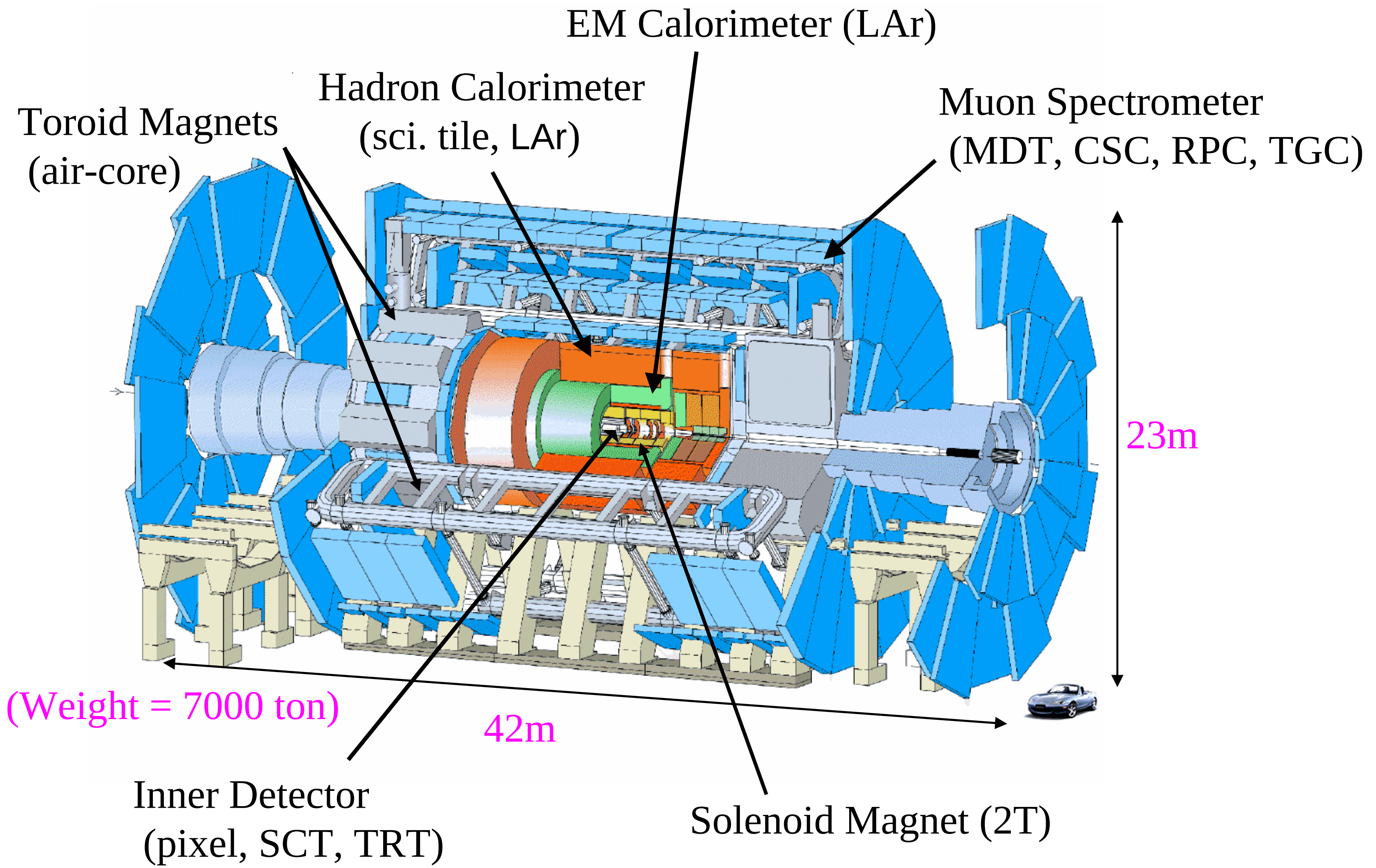

Compact Muon Solenoid (CMS)

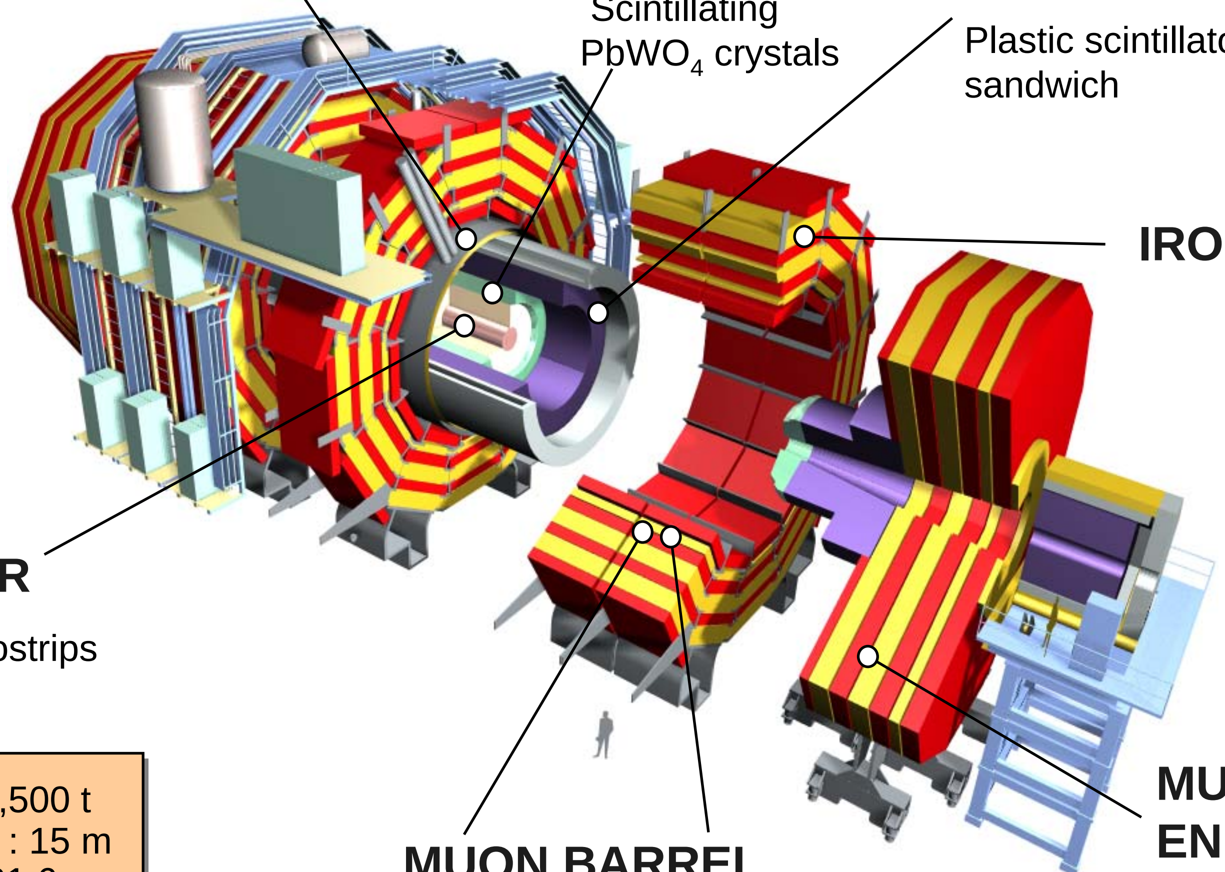

Total weight : 12,500 t
Overall diameter : 15 m
Overall length : 21.6 m
Magnetic field : 4 Tesla

ATLAS Inner Detector

Physics TDR
(1999)

Table 1-2 Parameters of the Inner Detector. The resolutions quoted are typical values (the actual resolution in each detector depends on the impact angle).

System	Position	Area (m^2)	Resolution σ (μm)	Channels (10^6)	η coverage
Pixels	1 removable barrel layer (B-layer) **R=4cm**	0.2	$R\phi = 12, z = 66$ **50μ(Rϕ)×300μ(Z)**	16	± 2.5
	2 barrel layers **R=11, 20cm**	1.4	$R\phi = 12, z = 66$	81	± 1.7
	5 end-cap disks on each side	0.7	$R\phi = 12, R = 77$	43	1.7–2.5
Silicon strips	4 barrel layers **R=30, 37,45,52cm**	34.4	**80μ pitch, 40mrad stereo** $R\phi = 16, z = 580$	3.2	± 1.4
	9 end-cap wheels on each side	26.7	$R\phi = 16, R = 580$	3.0	1.4–2.5
TRT	Axial barrel straws **R=56～107cm**		**4mmϕ straw** 170 (per straw)	0.1	± 0.7
	Radial end-cap straws		170 (per straw)	0.32	0.7–2.5
	36 straws per track				

(→ ～30μ, continuous tracking, electron-id)

ATLAS Inner Detector

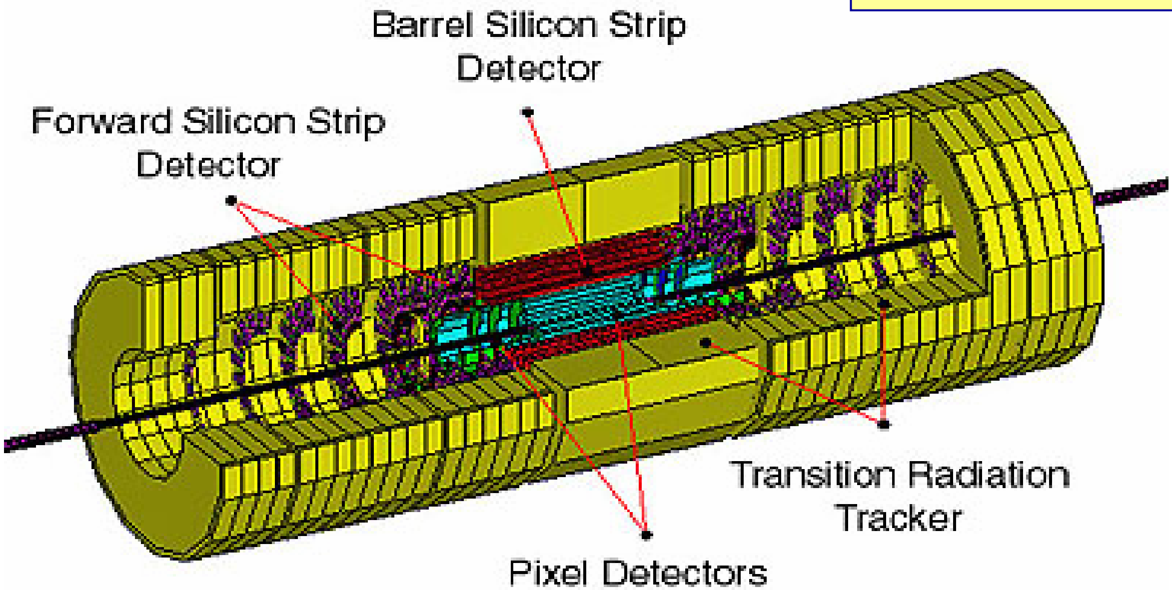

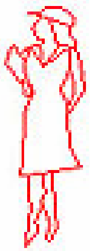

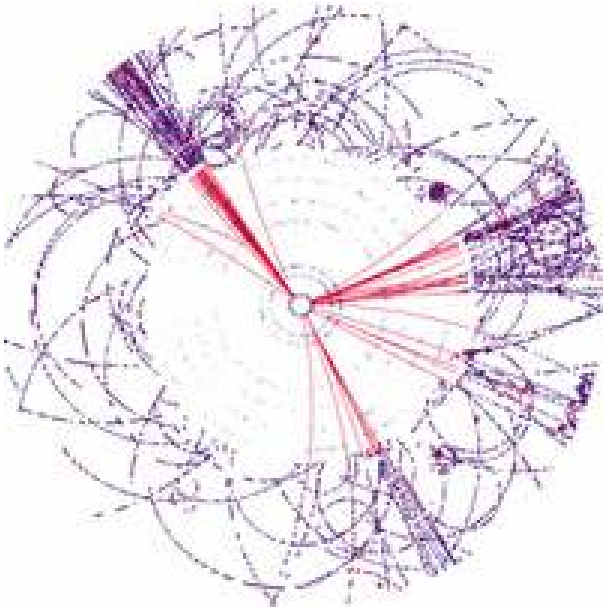

- **Solenoid Magnet (2T field)**
- Pixel Detectors (1.4×10^8channels)
- Strip Detectors (6×10^6 channels)
- Transition Radiation Tracker (4×10^5 channels)

➔ $\sigma(p_T)/p_T \sim 0.4\ p_T$ (p_T in TeV)

CMSとの比較

ATLAS Barrel Inner Detector

$H \rightarrow ZZ^* \rightarrow \mu^+\mu^-e^+e^-$ (m_H = 130 GeV)

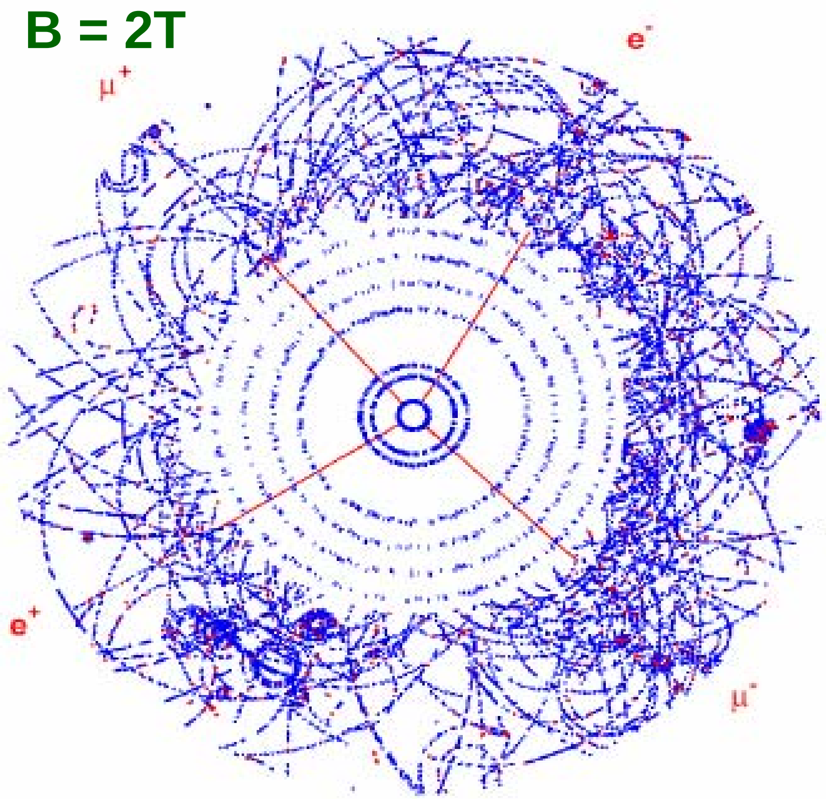

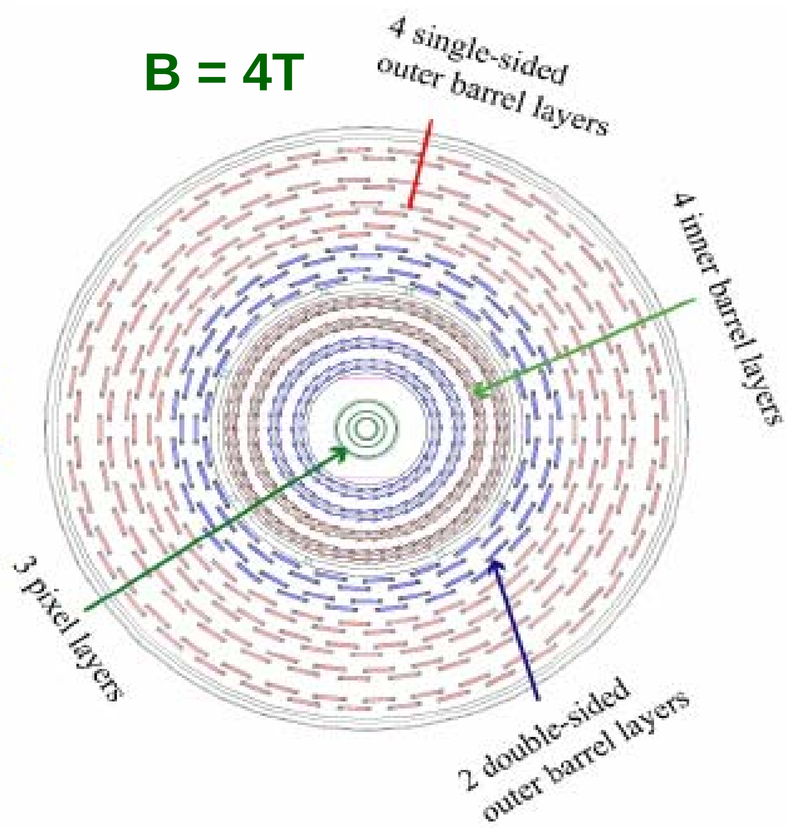

$\sigma(p_T)/p_T \sim 0.36\, p_T + 0.013$ (p_T in TeV) $\sim 0.15\, p_T + 0.005$

Figure 1-ii Event display of the process $H \rightarrow ZZ^* \rightarrow \mu^+\mu^-e^+e^-$ in the barrel part of the Inner Detector.

(ATLASはK_S−idも可)

Tracking ??

アトラス実験 Liq.Ar and Tile Calorimeters

IDやLiq.Arの読み出しケーブルやサービスなどのため物質量が非常に多い（η〜1.5）。

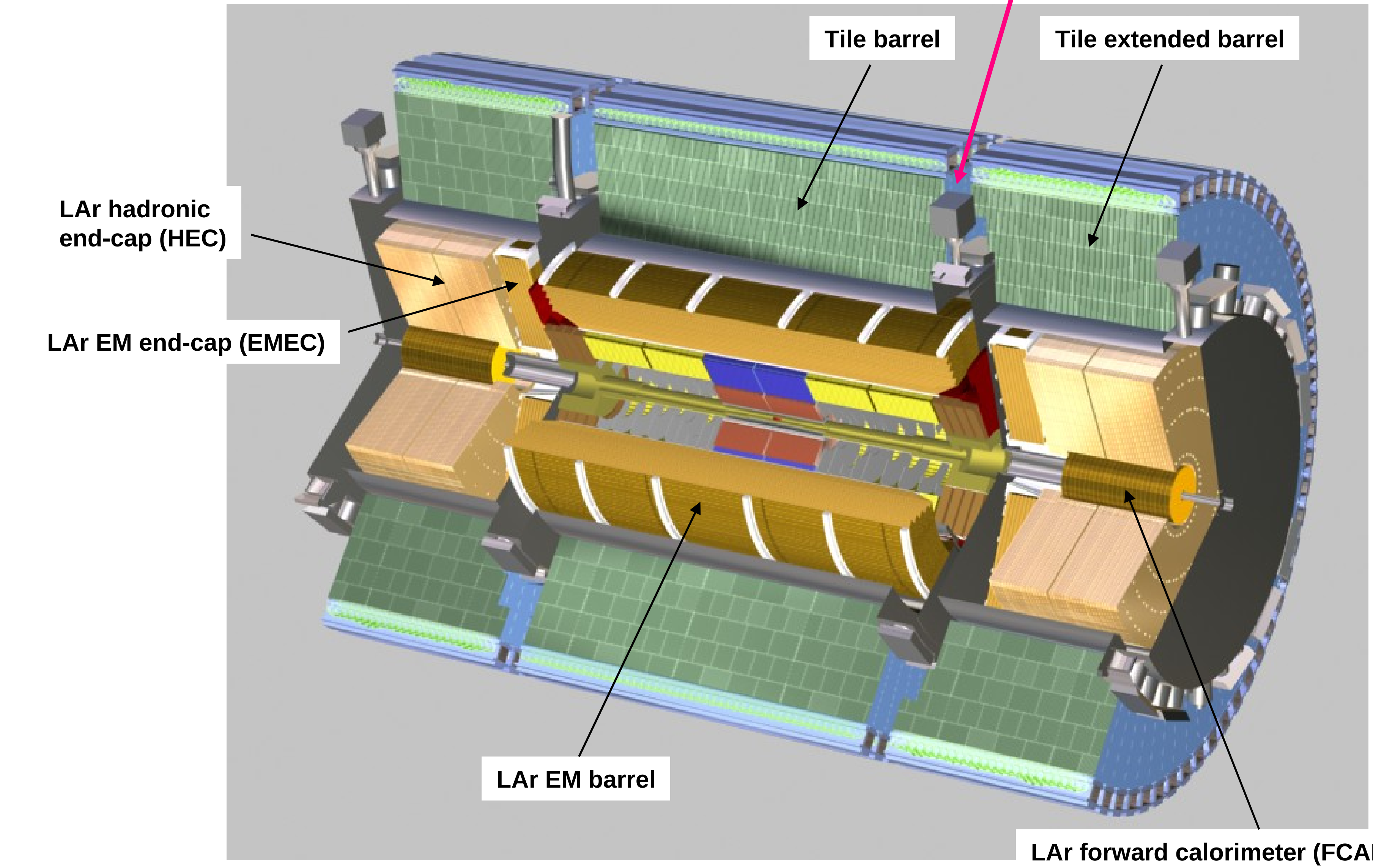

ATLAS EM Calorimeter

Table 1-3 Pseudorapidity coverage, granularity and longitudinal segmentation of the ATLAS calorimeters.

EM CALORIMETER		Barrel	End-cap	
Coverage		$\lvert\eta\rvert < 1.475$	$1.375 < \lvert\eta\rvert < 3.2$	
Longitudinal segmentation		3 samplings	3 samplings	$1.5 < \lvert\eta\rvert < 2.5$
			2 samplings	$1.375 < \lvert\eta\rvert < 1.5$
				$2.5 < \lvert\eta\rvert < 3.2$
Granularity ($\Delta\eta\times\Delta\phi$)				
Sampling 1	$4\ X_0$	0.003×0.1	0.025×0.1	$1.375 < \lvert\eta\rvert < 1.5$
			0.003×0.1	$1.5 < \lvert\eta\rvert < 1.8$
			0.004×0.1	$1.8 < \lvert\eta\rvert < 2.0$
			0.006×0.1	$2.0 < \lvert\eta\rvert < 2.5$
			0.1×0.1	$2.5 < \lvert\eta\rvert < 3.2$
Sampling 2	$16\ X_0$	0.025×0.025	0.025×0.025	$1.375 < \lvert\eta\rvert < 2.5$
			0.1×0.1	$2.5 < \lvert\eta\rvert < 3.2$
Sampling 3	$2\sim12\ X_0$	0.05×0.025	0.05×0.025	$1.5 < \lvert\eta\rvert < 2.5$
PRESAMPLER		**Barrel**	**End-cap**	
Coverage		$\lvert\eta\rvert < 1.52$	$1.5 < \lvert\eta\rvert < 1.8$	
Longitudinal segmentation		1 sampling	1 sampling	
Granularity ($\Delta\eta\times\Delta\phi$)		0.025×0.1	0.025×0.1	

- "preshower" detector for particle id.(γ/π^0, e/π)
- precise η position measurement

for energy loss correction

Barrel EM calorimeter

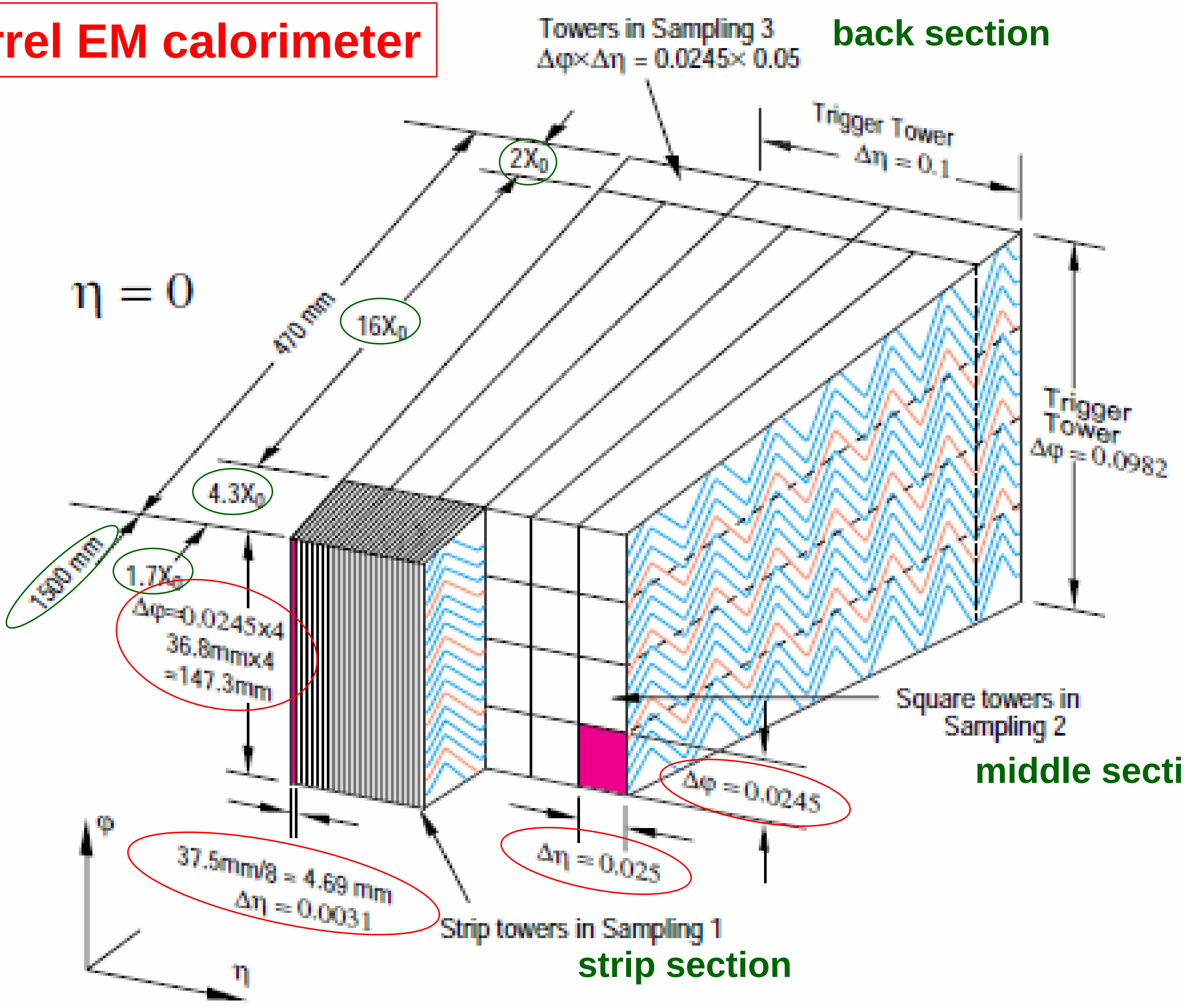

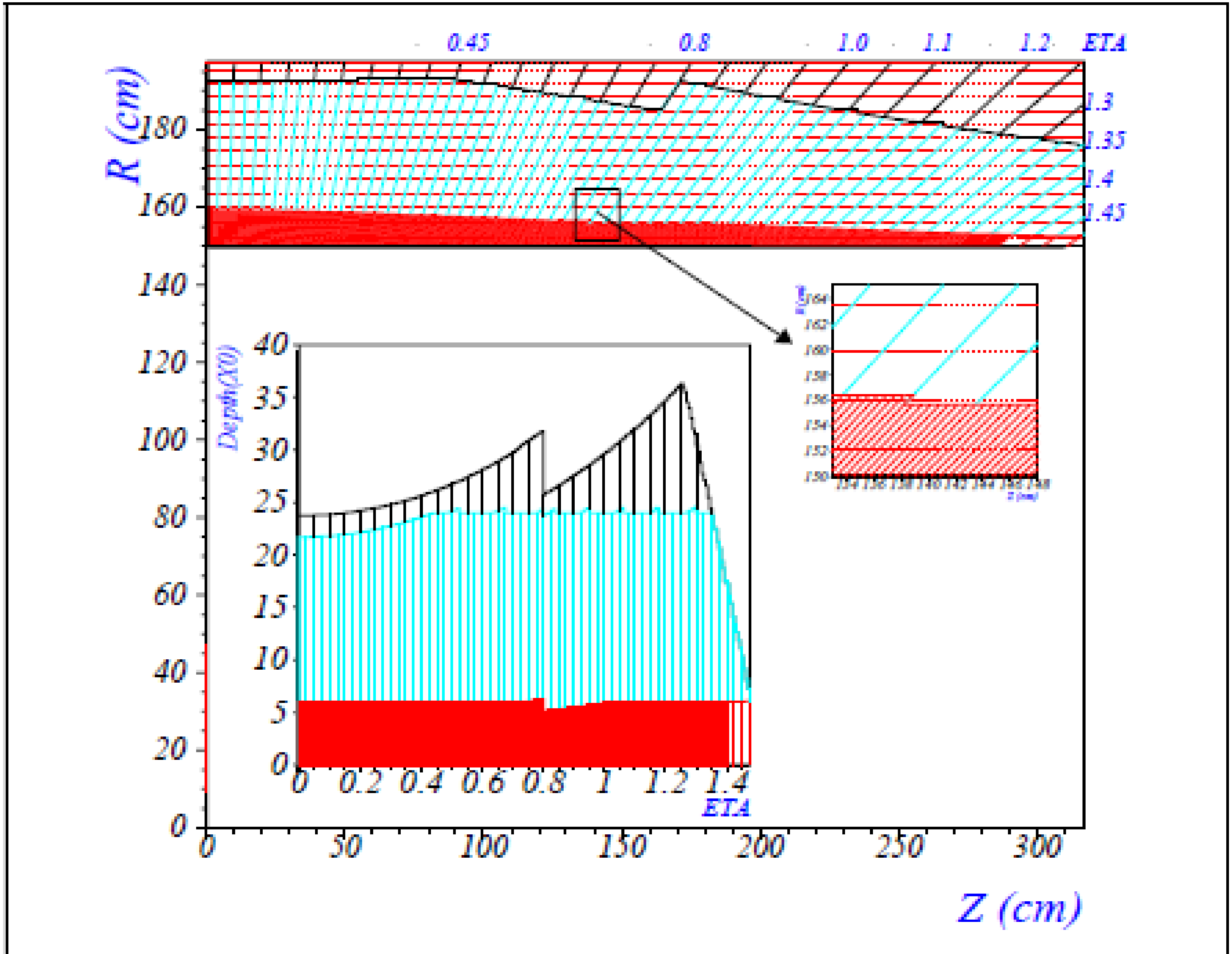

Figure 2-16 Segmentation of the barrel EM calorimeter. The bottom plot shows the thicknesses (in radiation lengths) up to the end of the three samplings (upstream material included).

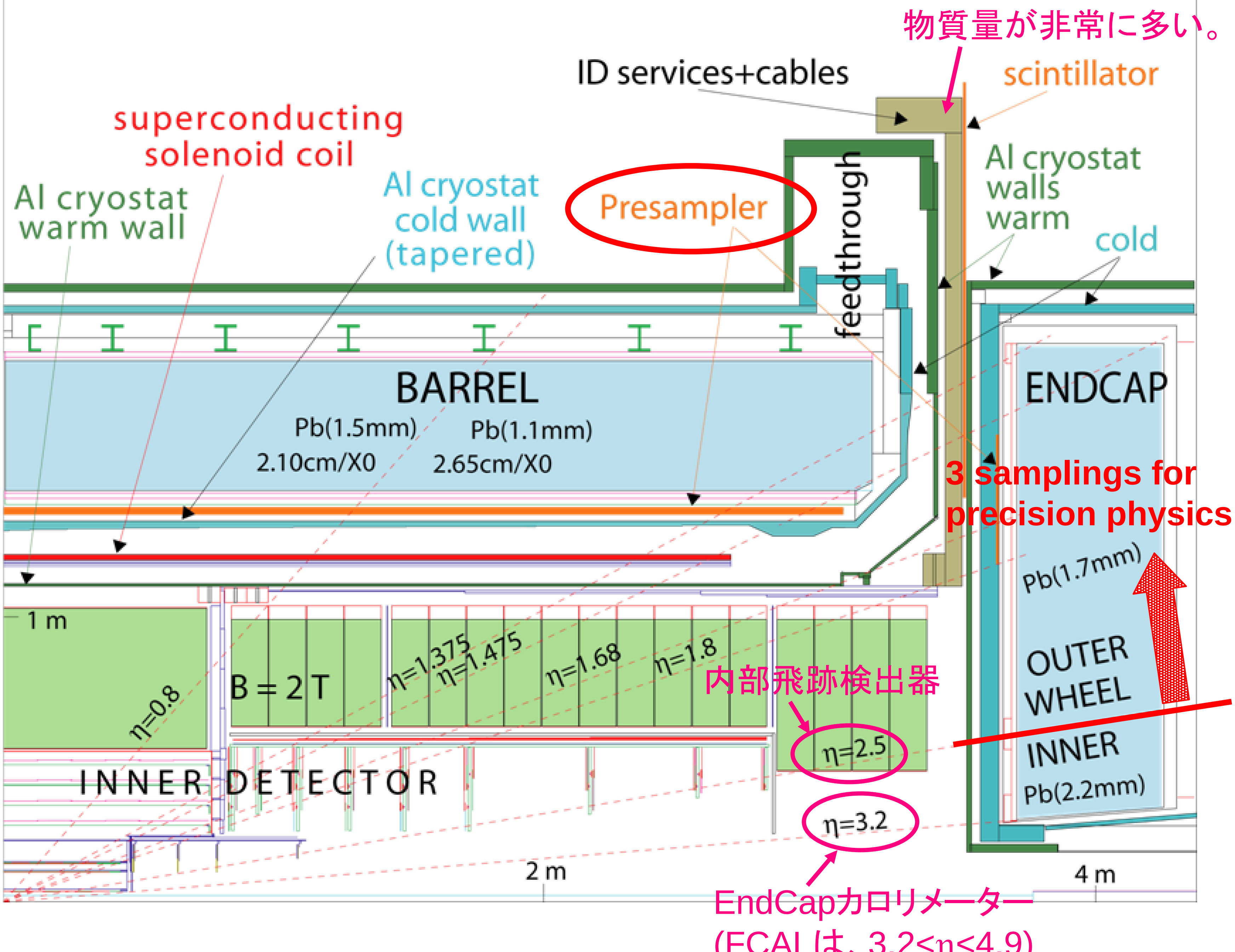
物質量が非常に多い。
ID services+cables
scintillator
superconducting solenoid coil
Al cryostat warm wall
Al cryostat cold wall (tapered)
Presampler
feedthrough
Al cryostat walls warm
cold
BARREL
Pb(1.5mm)
Pb(1.1mm)
2.10cm/X0
2.65cm/X0
ENDCAP
3 samplings for precision physics
Pb(1.7mm)
OUTER WHEEL
INNER
Pb(2.2mm)
1 m
B = 2 T
η=0.8
η=1.375
η=1.475
η=1.68
η=1.8
内部飛跡検出器
η=2.5
η=3.2
INNER DETECTOR
2 m
4 m
EndCapカロリメーター
(FCALは、3.2<η<4.9)

EM Calorimeter Performance

物理のベンチマーク・プロセス　H→$\gamma\gamma$、$4e^{\pm}$

検出器　… 4元運動量（E,**p**） or (t,**x**)を測定するのが良い。例：Kamiokande

ATLAS Liquid Argon カロリメーターは、これが出来る！

- エネルギー分解能　　**$\sigma/E = 10\%/\sqrt{E} \oplus 200(400)\mathrm{MeV}/E \oplus 0.7\%$**
- 角度分解能　　**4-6 mrad/√E** （φ方向、Middle Layer(第2層)）
  50 mrad/√E （η方向、Strip+Middle Layer→Z vertexの測定）
- 時間分解能　　**100 ps** (1ns at 1GeV)
- 粒子識別　　$e^{\pm}$/jets, γ/π^0 > 3 at E_T=50GeV
- Linearity　　< 0.1%
- Dynamic range　　20MeV(MIP粒子μも検出可能) - 2TeV（余剰次元などの信号）

$\sigma_{x,y}$(IP) ～ 15μ

σ_z(IP) ～ 5.6cm

- ATLAS Liquid Argonカロリメーター
  - 鉛／液体アルゴンのサンプリング・カロリメーター（アコーディオン型）
  - Azimuthal角＝2π（クラック無し）、擬ラピディティー η<3.2 (FCAL <4.9)をカバー。
  - Liquid Argonは、intrinsicにrad-hard。
  - アコーディオン・ジオメトリー

CMS ECAL $PbWO_4$

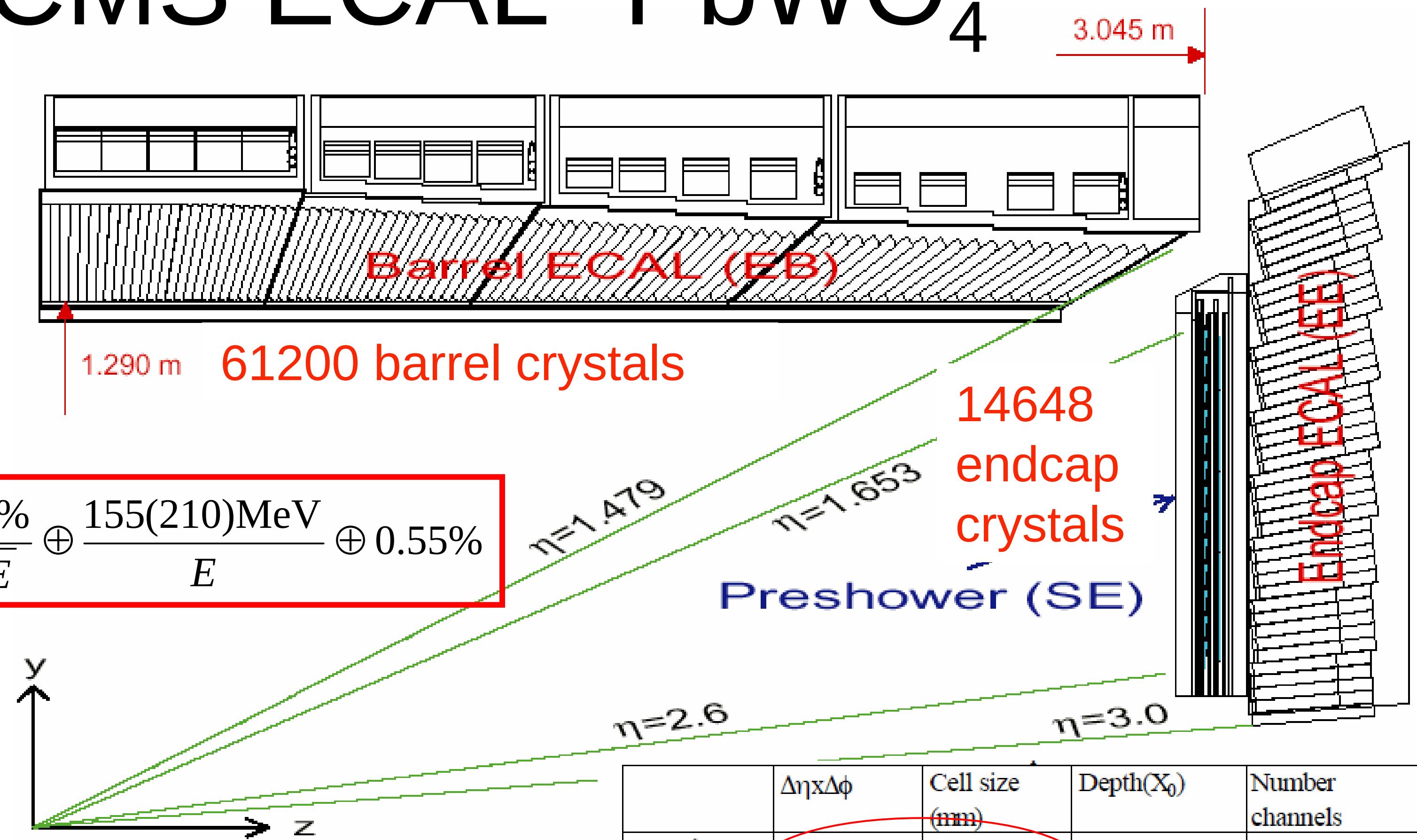

$$\frac{\sigma_E}{E} = \frac{2.7\%}{\sqrt{E}} \oplus \frac{155(210)\text{MeV}}{E} \oplus 0.55\%$$

$$\frac{\sigma_E}{E} = \frac{10\%}{\sqrt{E}} \oplus \frac{200(400)\text{MeV}}{E} \oplus 0.7\%$$

ATLAS

	ΔηxΔφ	Cell size (mm)	Depth(X_0)	Number of channels
Barrel η<1.48	0.0175 x 0.0175	21.8 x 21.8	25.8	61200
Endcap 1.48<η<3.0	variable	29.6x29.6	23	15632
End-cap preshower 1.65<η<2.6		63 x 1.9	3	~130000

ATLAS Hadron Calorimeter

- >11λ in front of Muon system → reduction of punch−through
- ~10λ active calorimeter(incl. 1.2λ of EM) → good E−res. for HE jets

HADRONIC TILE	Barrel	Extended barrel	
Coverage	$\|\eta\| < 1.0$	$0.8 < \|\eta\| < 1.7$	
Longitudinal segmentation	3 samplings	3 samplings	
Granularity ($\Delta\eta \times \Delta\phi$)			
Samplings 1 and 2	0.1×0.1	0.1×0.1	
Sampling 3	0.2×0.1	0.2×0.1	
HADRONIC LAr		**End-cap**	
Coverage		$1.5 < \|\eta\| < 3.2$	
Longitudinal segmentation		4 samplings	
Granularity ($\Delta\eta \times \Delta\phi$)		0.1×0.1	$1.5 < \|\eta\| < 2.5$
		0.2×0.2	$2.5 < \|\eta\| < 3.2$
FORWARD CALORIMETER		**Forward**	
Coverage	LAr, rod + tube geometry	$3.1 < \|\eta\| < 4.9$	
Longitudinal segmentation		3 samplings	
Granularity ($\Delta\eta \times \Delta\phi$)		$\sim 0.2 \times 0.2$	

TileCal

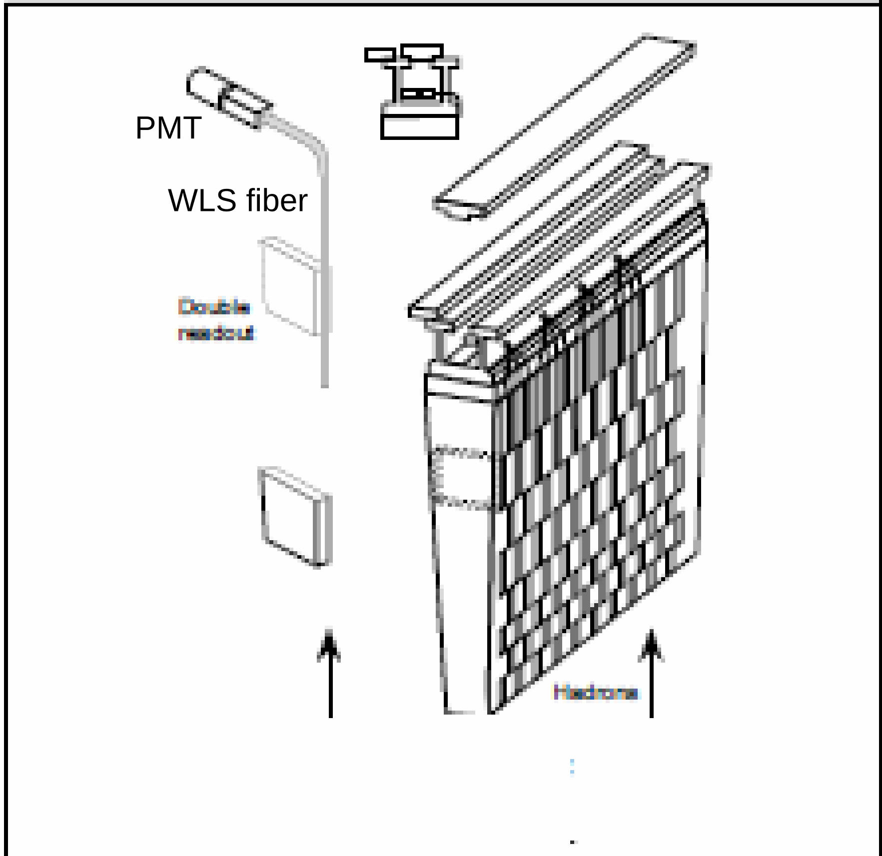

Figure 1-5 The principle of the Tile calorimeter design.

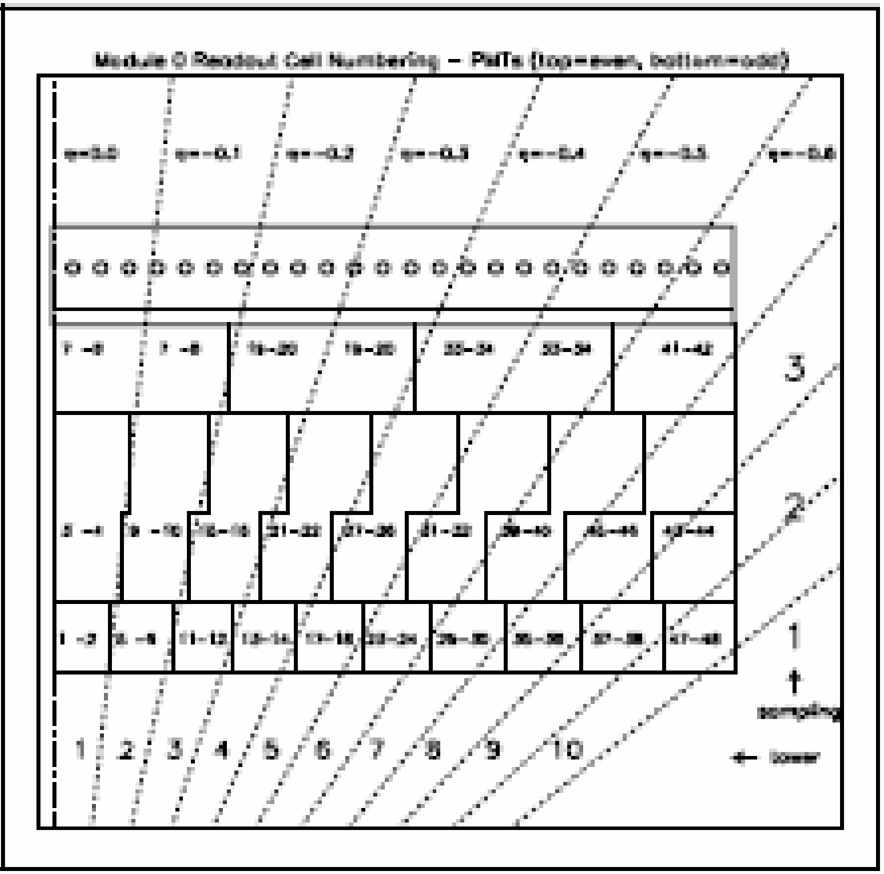

Figure 1-6 The layout of half a barrel module. The fibres are grouped such that the three samplings approximate η boundaries from |η|<1. The numbers inside the cells correspond to the PMTs to which each cell is connected.

～10k channels

FCAL

(~9.5λ)

LAr gap = 250μ, 375μ

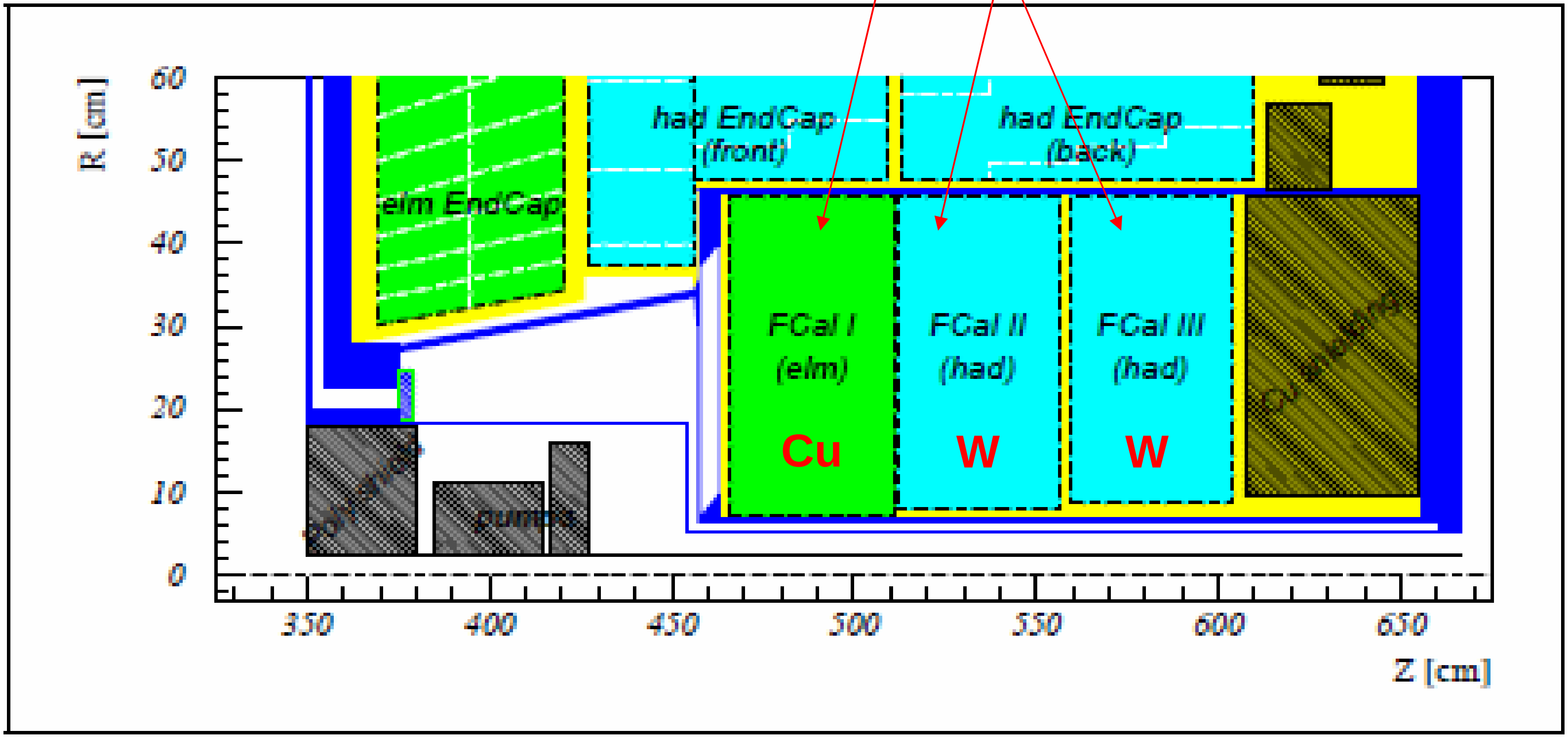

Figure 3-9 A longitudinal cross-section through the FCAL, and the surrounding region, according to the geometry used in the simulation program. The light grey areas indicate calorimeter elements that contain LAr as the active medium. The black areas depict the cryostat walls and support structures.

FCAL

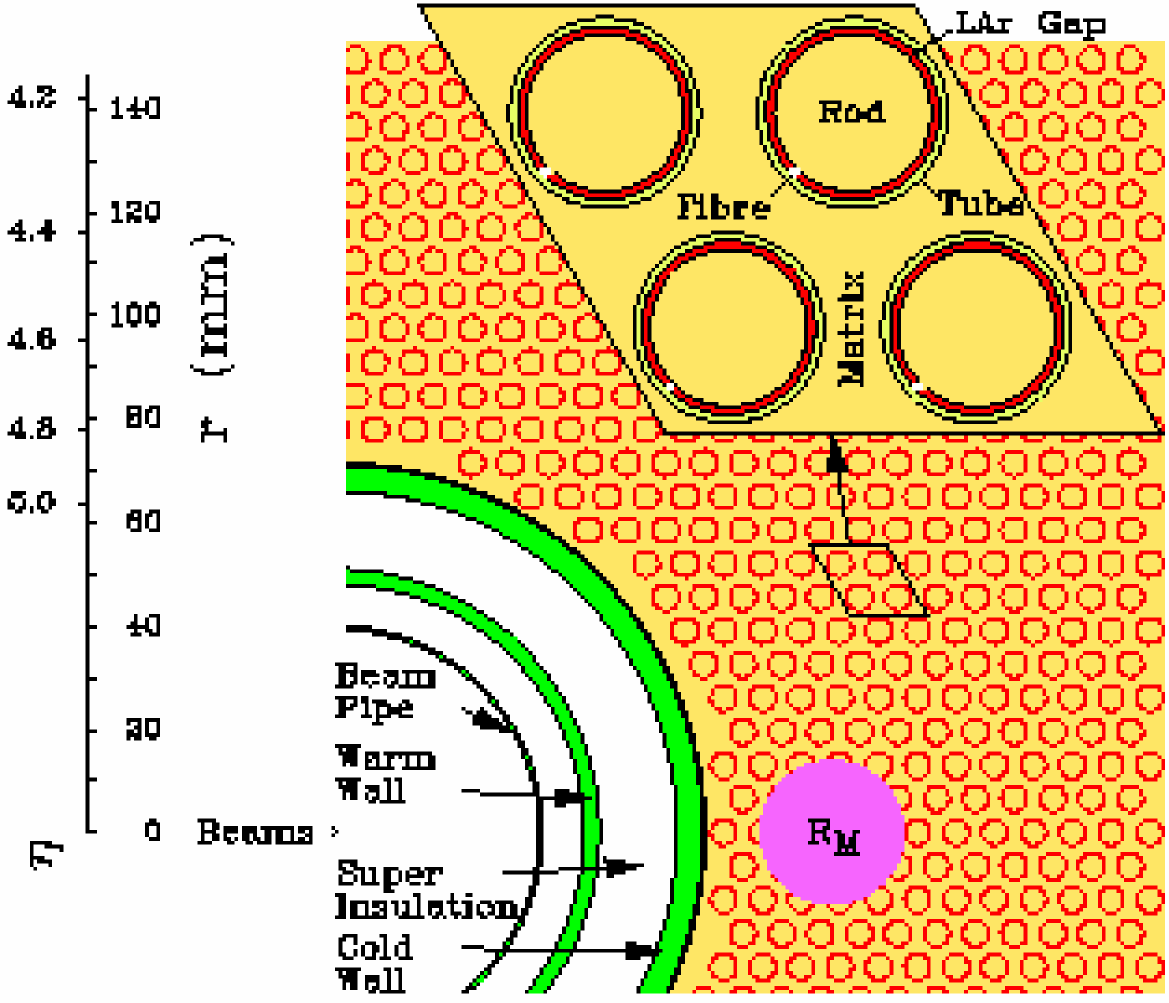

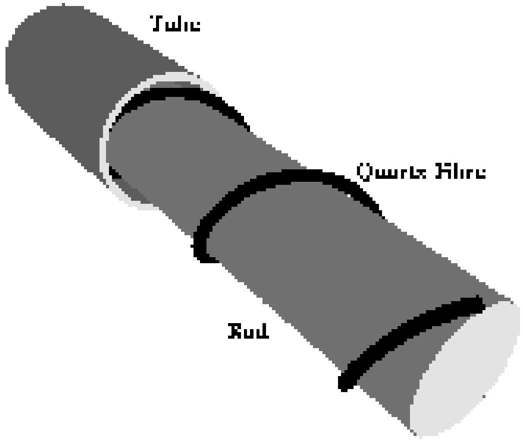

4 rod are ganged for readout → 4k channels

The ATLAS Muon Spectrometer

ATLAS: A Toroidal LHC ApparatuS

Muon Spectrometer:

- toroidal magnetic field: <B> = 4 Tm
  $\Rightarrow$ high p_t-resolution independent of the polar angle
- size defined by large lever arm to allow high stand-alone precision
- air-core coils to minimise the multiple scattering
- 3 detector stations
  - cylindrical in barrel
  - wheels in end caps
- coverage: $|\eta| < 2.7$

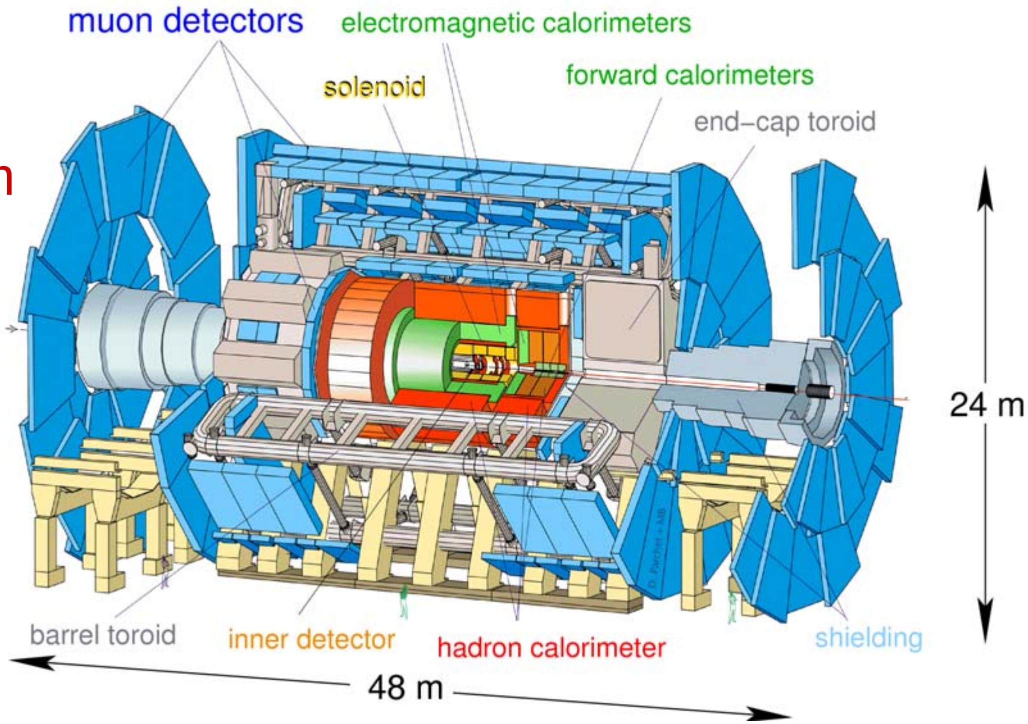

Trackers:

- fast trigger chambers: TGC, RPC
- high resolution tracking detectors: MDT,CSC

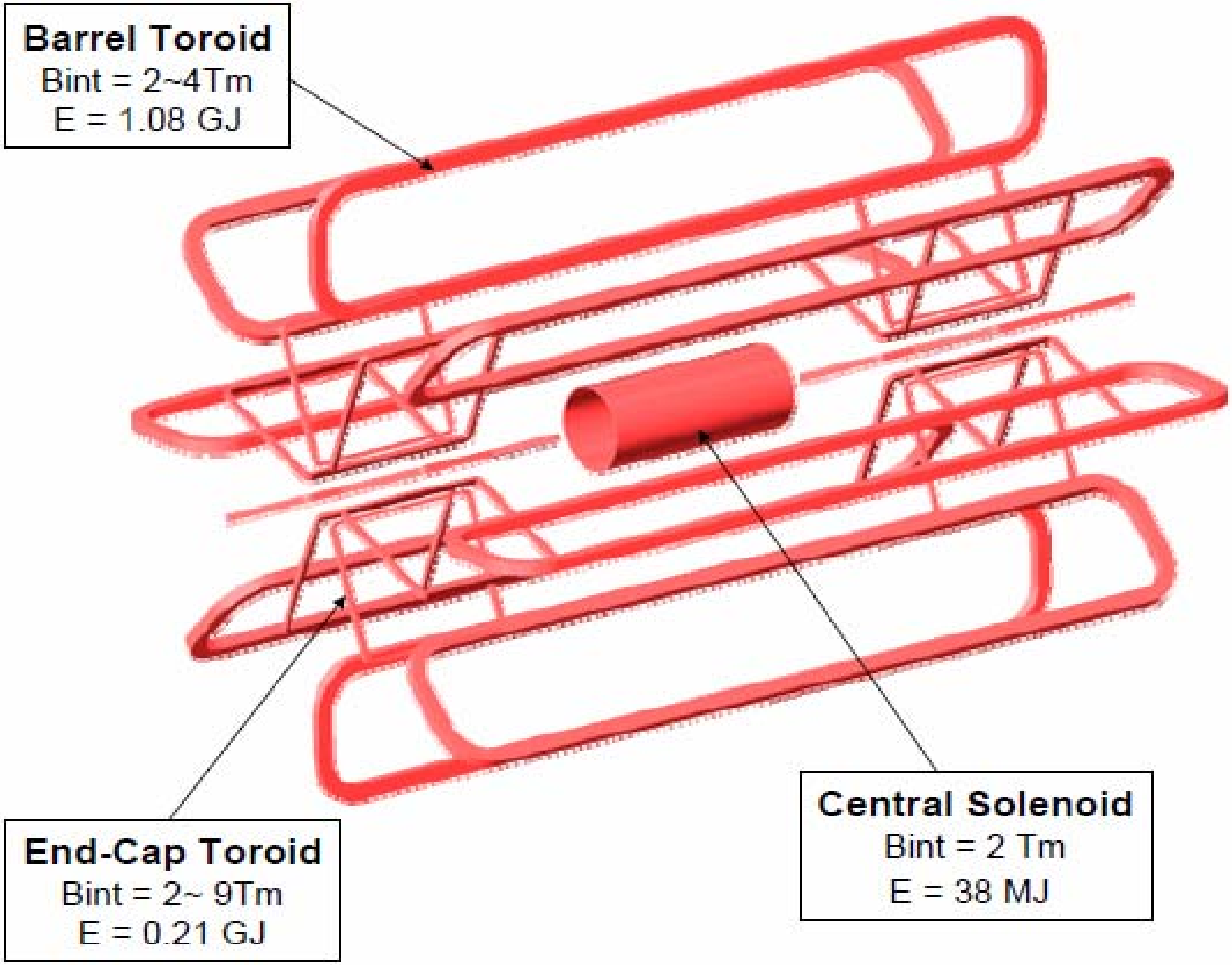
Barrel Toroid
Bint = 2~4Tm
E = 1.08 GJ
End-Cap Toroid
Bint = 2~ 9Tm
E = 0.21 GJ
Central Solenoid
Bint = 2 Tm
E = 38 MJ

Muon Detection and Magnet System

ATLAS A Toroidal LHC ApparatuS

CMS Compact Muon Solenoid

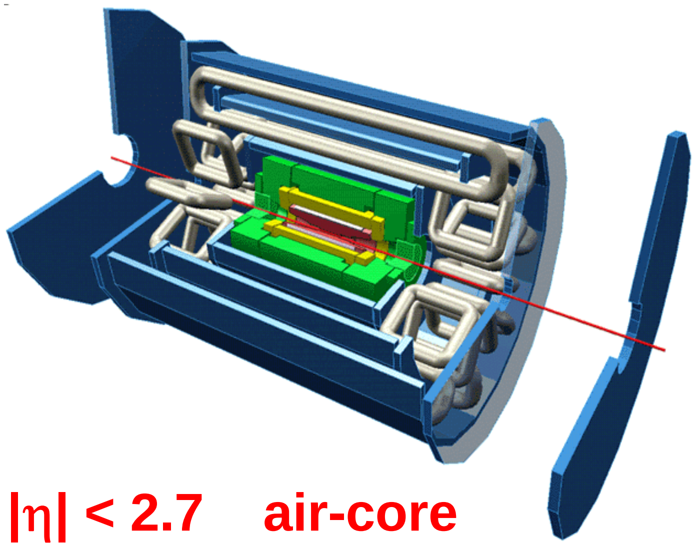

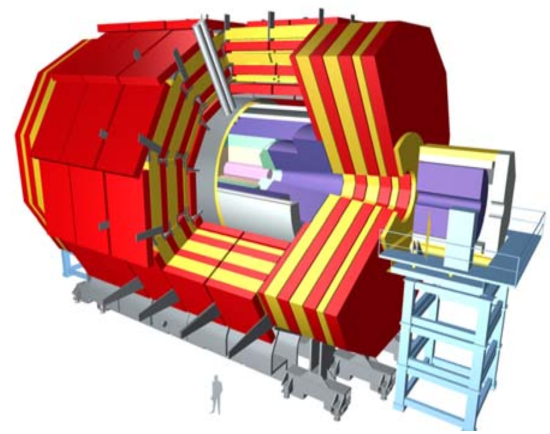

|η| < 2.7 air-core

|η| < 2.4 Fe

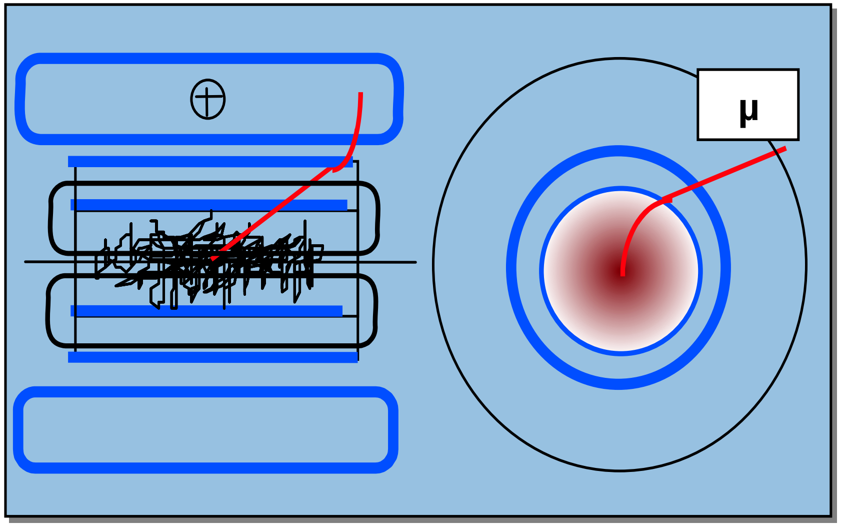

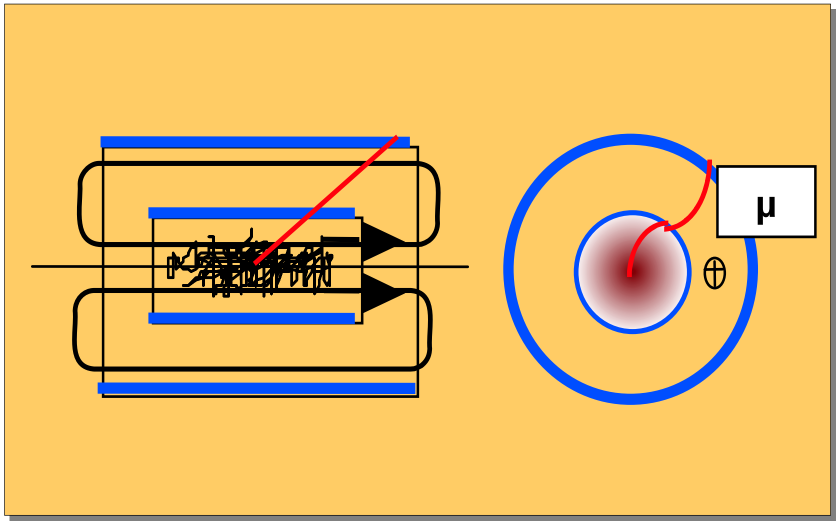

Muon Detector

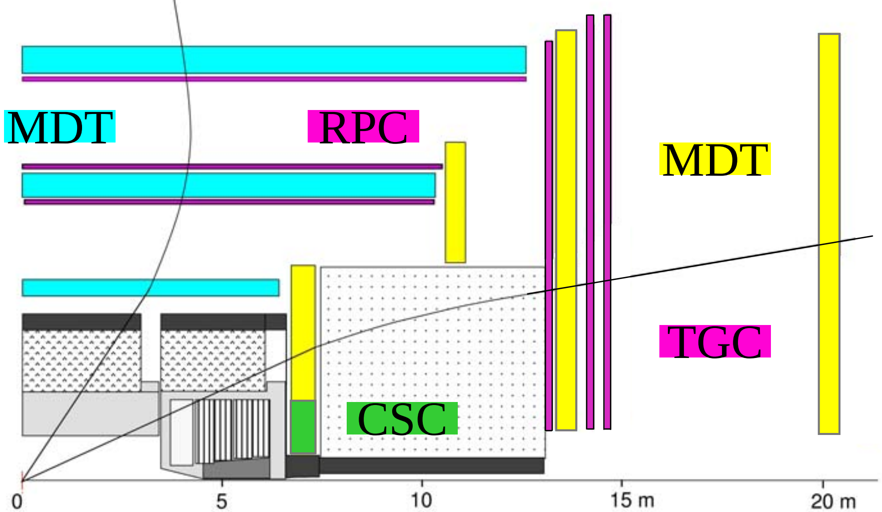

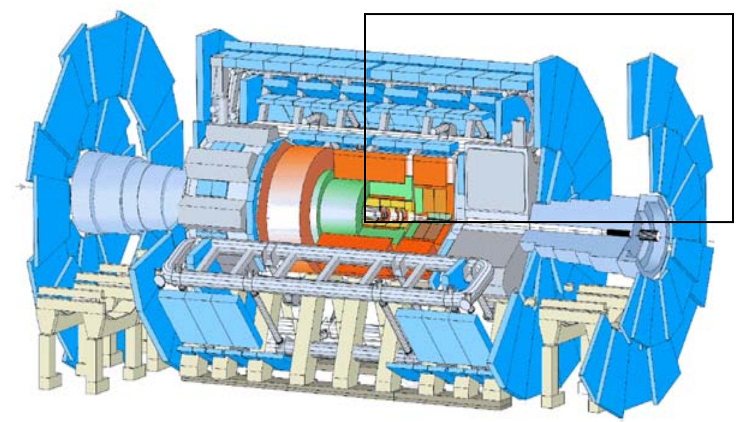

Precision chambers

(p-meas.)

Monitored **D**rift **T**ubes ($|\eta| < 2$)

with a single wire resolution of 80 μm

Cathode **S**trip **C**hambers ($2 < |\eta| < 2.7$)

at higher particle fluxes

Trigger chambers

(trigger, 2-nd coord.)

Resistive **P**late **C**hambers ($|\eta| < 1.05$)

with a good time resolution of 1 ns

Thin **G**ap **C**hambers ($1.05 < |\eta| < 2.4$)

at higher particle fluxes

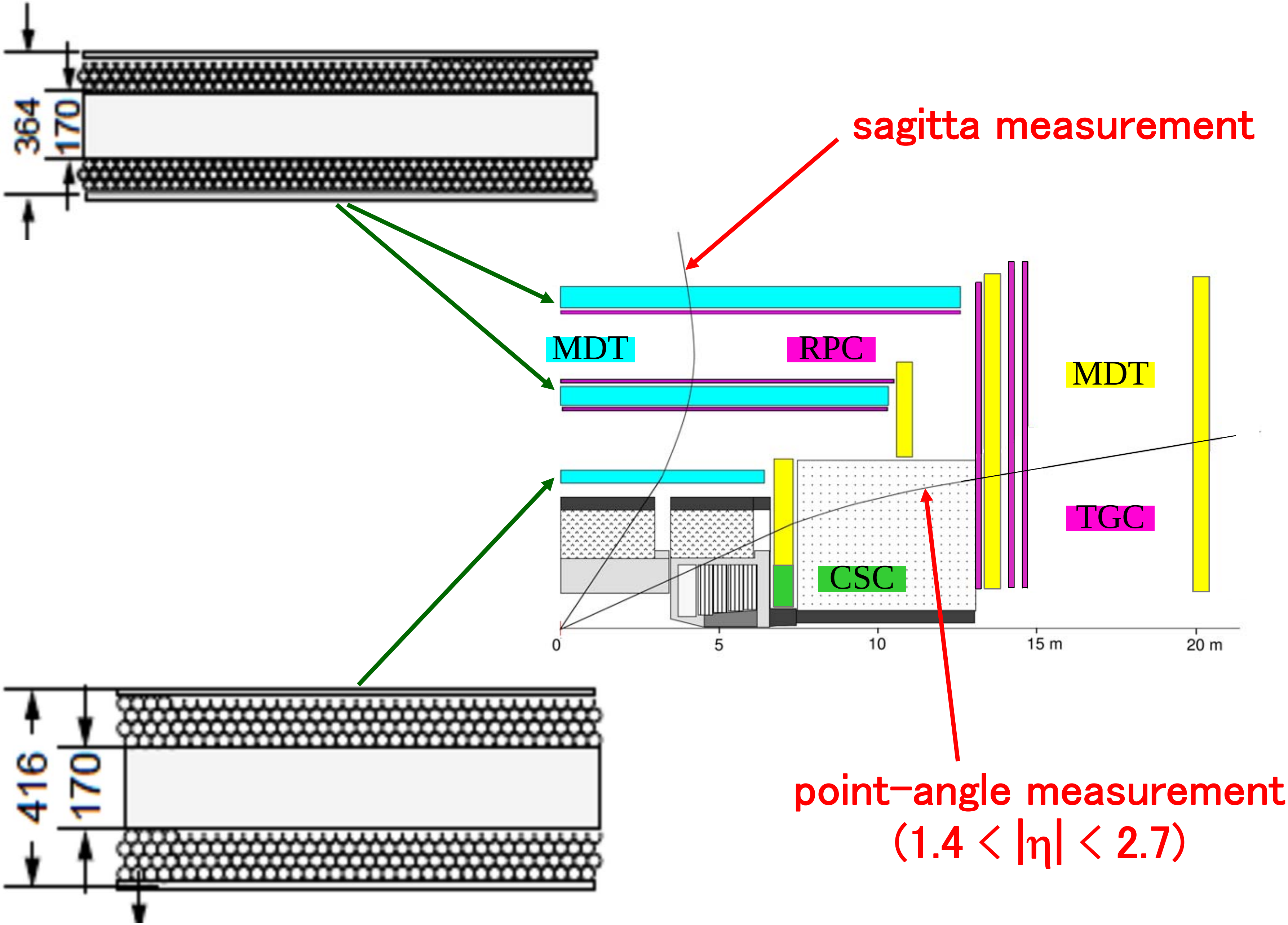

364
170
416
170
sagitta measurement
MDT
RPC
MDT
TGC
CSC
0
5
10
15 m
20 m
point-angle measurement
(1.4 < |η| < 2.7)

Momentum measurement

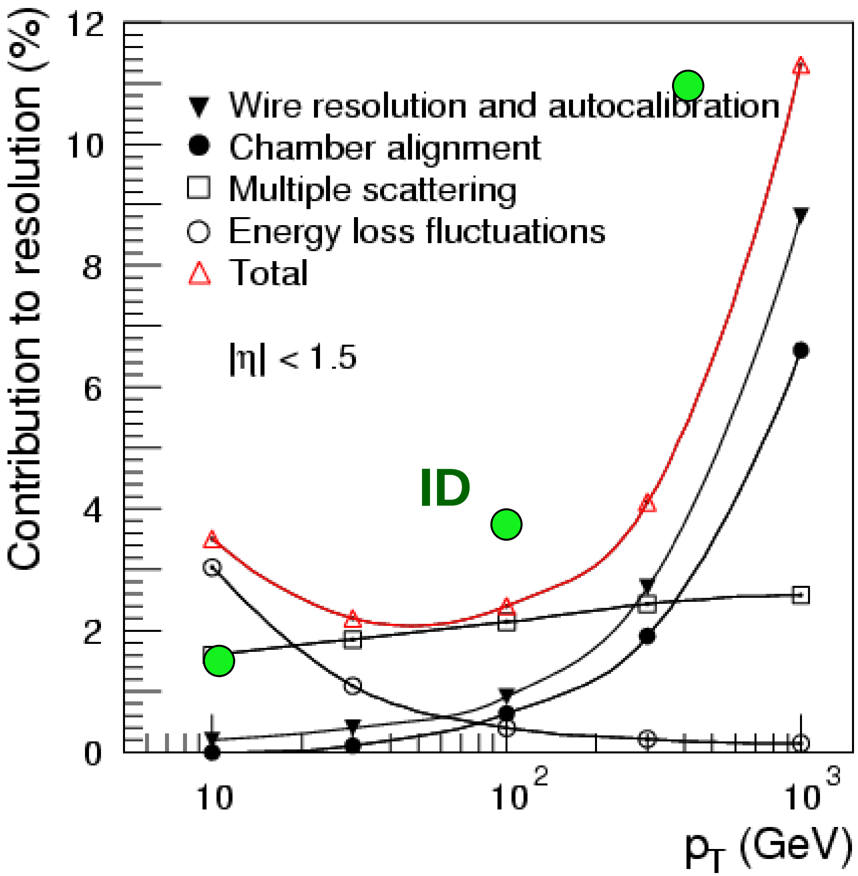

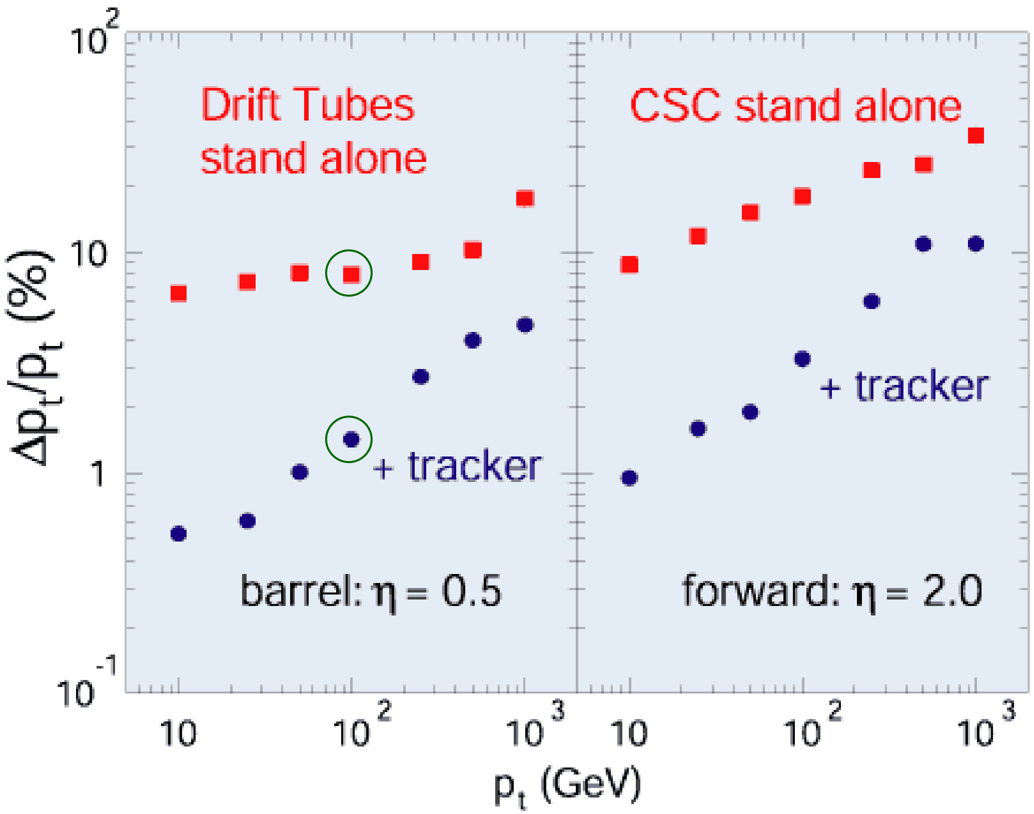

ATLAS		**CMS**
2.5 %@100GeV	← muon stand alone →	8 % @ 100GeV
3.8 %	← inner detector →	1.6 %

4 Muon final state

- $H \rightarrow \mu\mu\mu\mu$

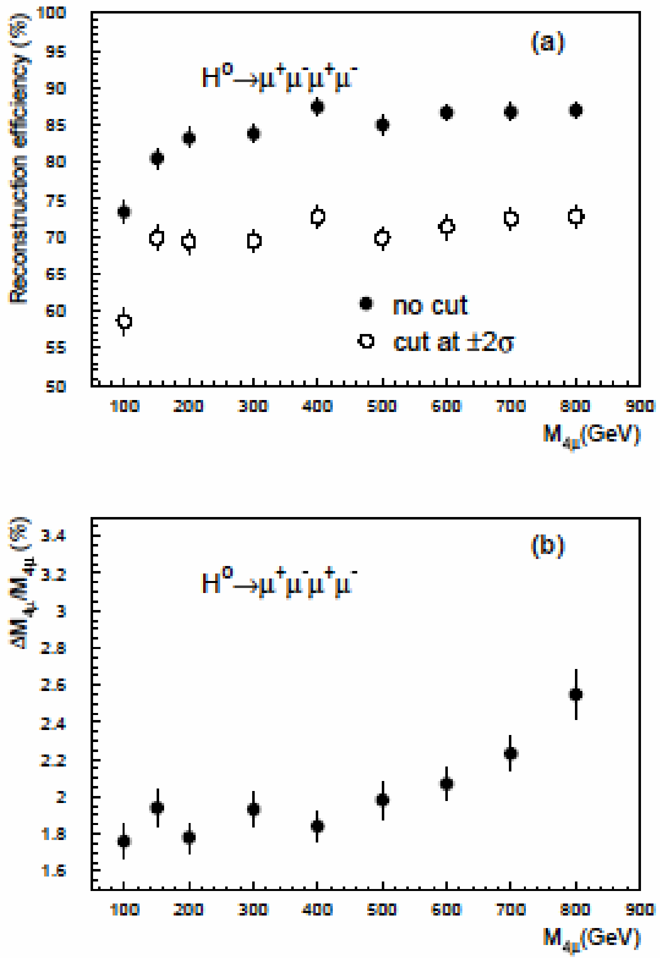

Figure 12-40 Four-muon reconstruction efficiency (a) and mass resolution (b) as a function of invariant mass. The reconstruction uses the muon spectrometer only; no Z mass constraint was applied.

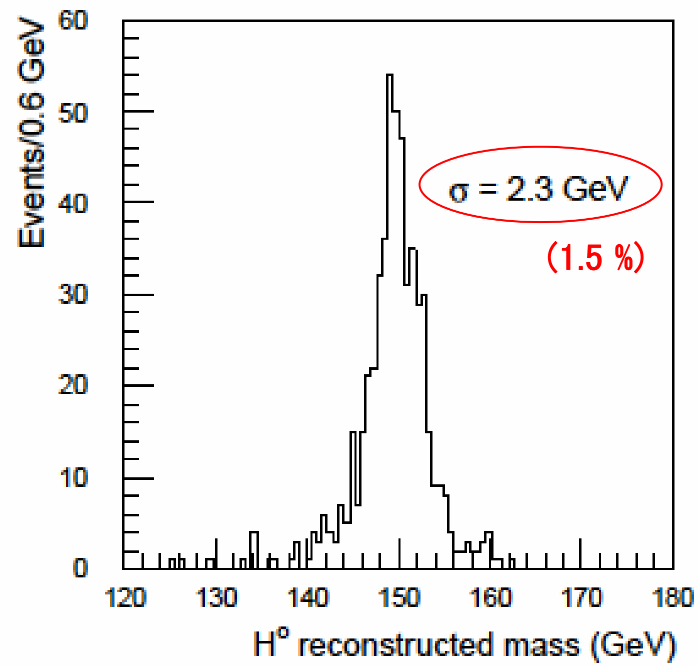

$\rightarrow \Gamma_H$

Figure 12-41 Reconstructed mass distribution for the Higgs decay $H^0 \rightarrow ZZ \rightarrow \mu^+\mu^- \mu^+ \mu^-$, constraining one muon pair to the Z mass.

Discovery Potential of SM Higgs

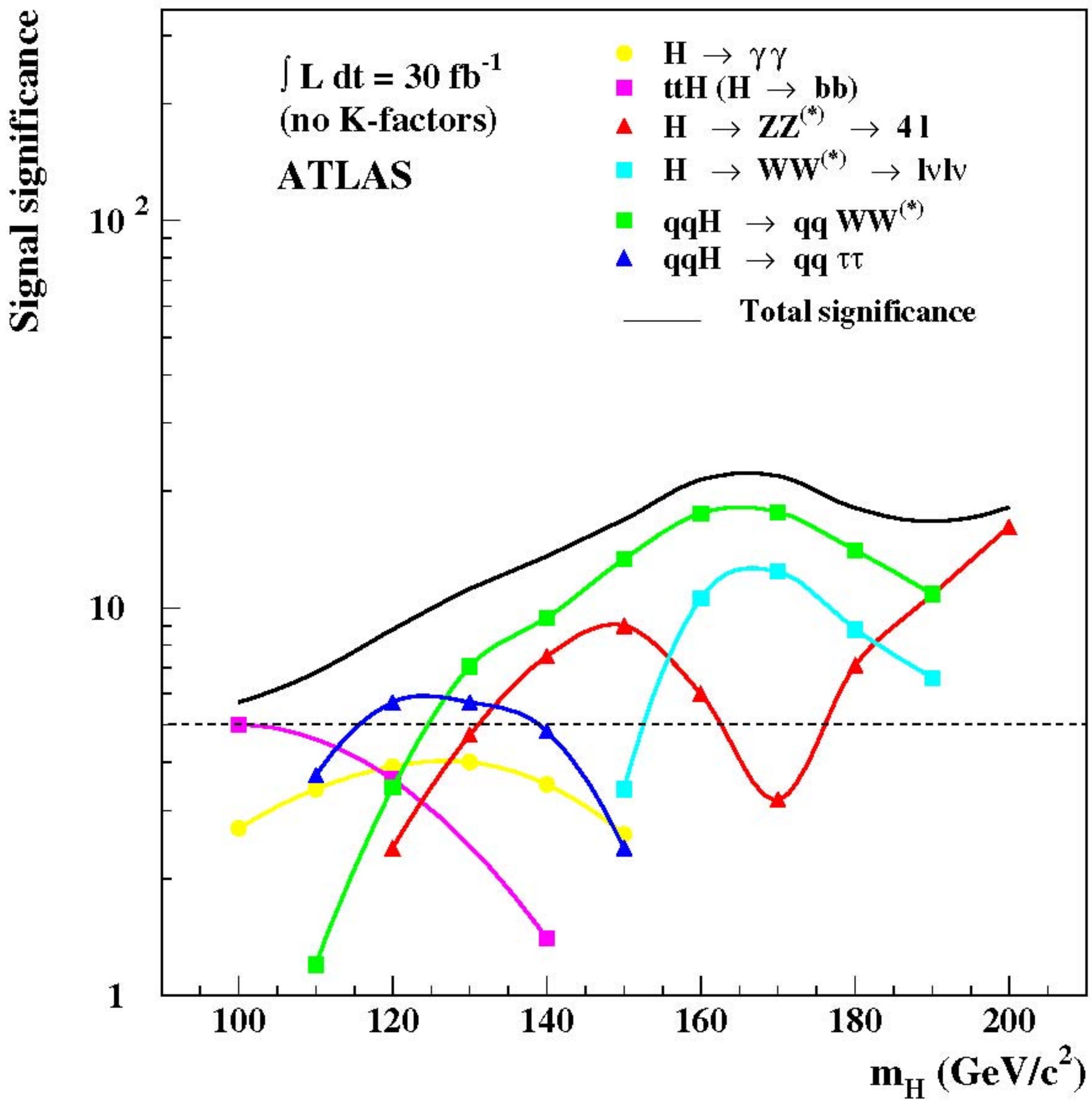

$H \rightarrow \gamma\gamma$

$$\frac{\sigma_M}{M} = \frac{1}{2}\left[\frac{\sigma_{E_1}}{E_1} \oplus \frac{\sigma_{E_2}}{E_2} \oplus \frac{\sigma_\theta}{\tan(\theta/2)}\right]$$

ATLAS

better uniformity and angular resolution

$$\frac{\sigma_E}{E} = \frac{10\%}{\sqrt{E}} \oplus \frac{200(400)\mathrm{MeV}}{E} \oplus 0.7\%$$

$$\sigma_\theta = \frac{50\mathrm{mrad}}{\sqrt{E}}$$

CMS

better energy resolution

$$\frac{\sigma_E}{E} = \frac{2.7\%}{\sqrt{E}} \oplus \frac{155(210)\mathrm{MeV}}{E} \oplus 0.55\%$$

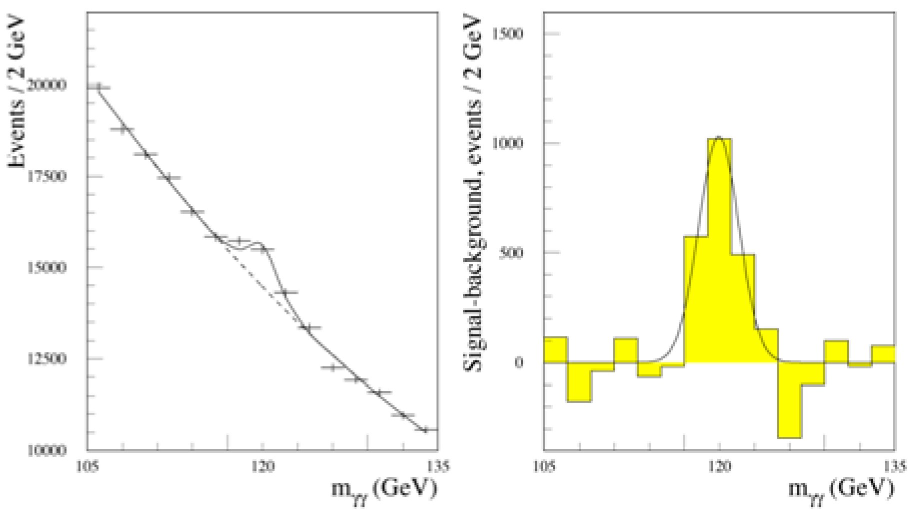

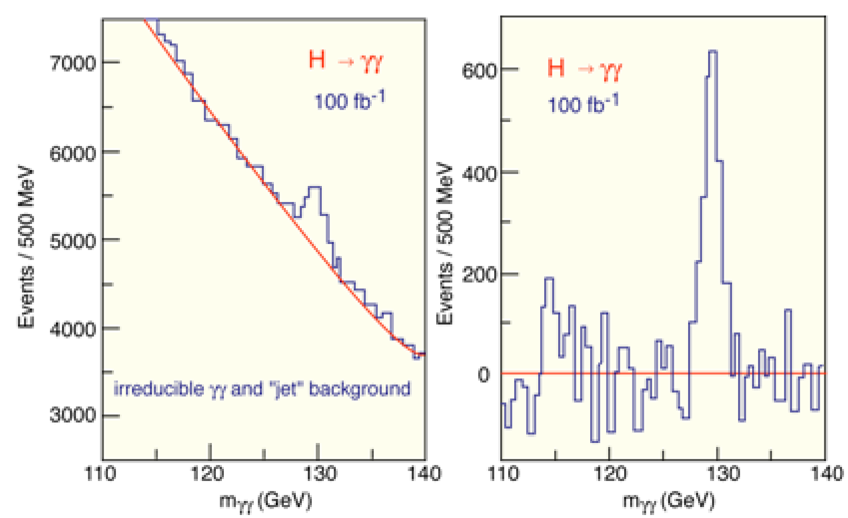

Combined $H\rightarrow\gamma\gamma$+0j and $H\rightarrow\gamma\gamma$+1j Analysis

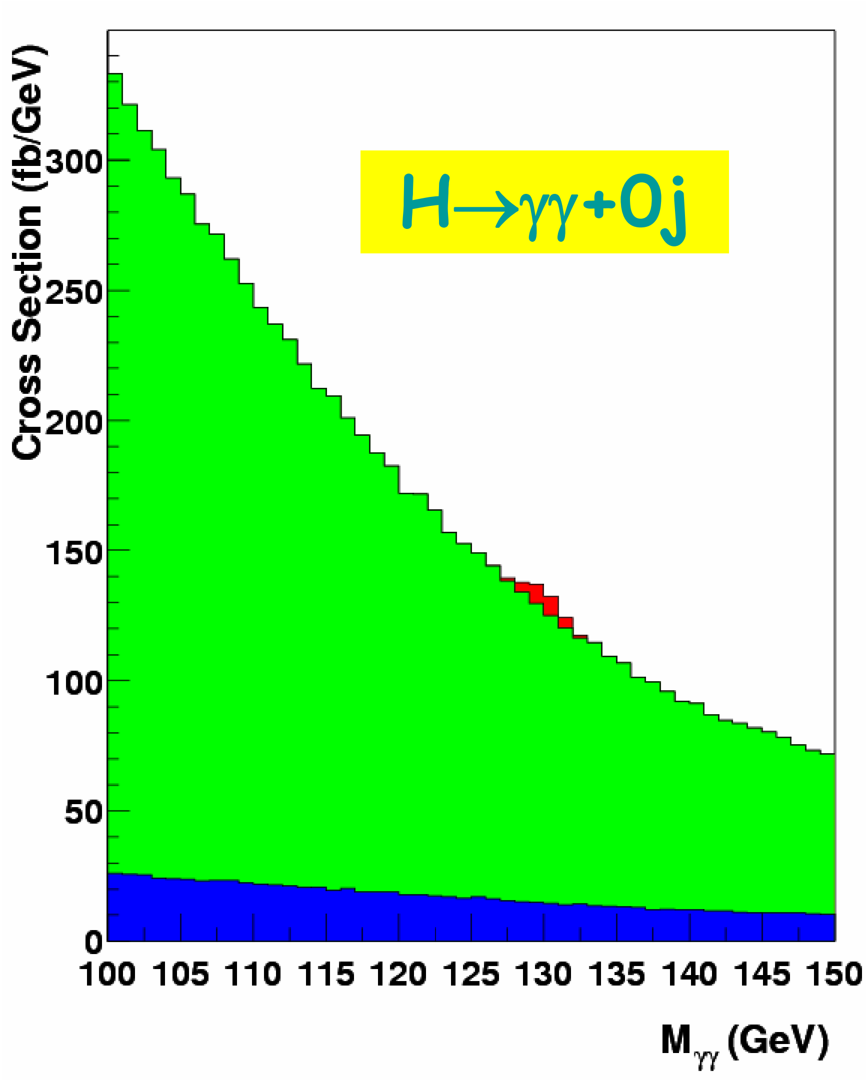

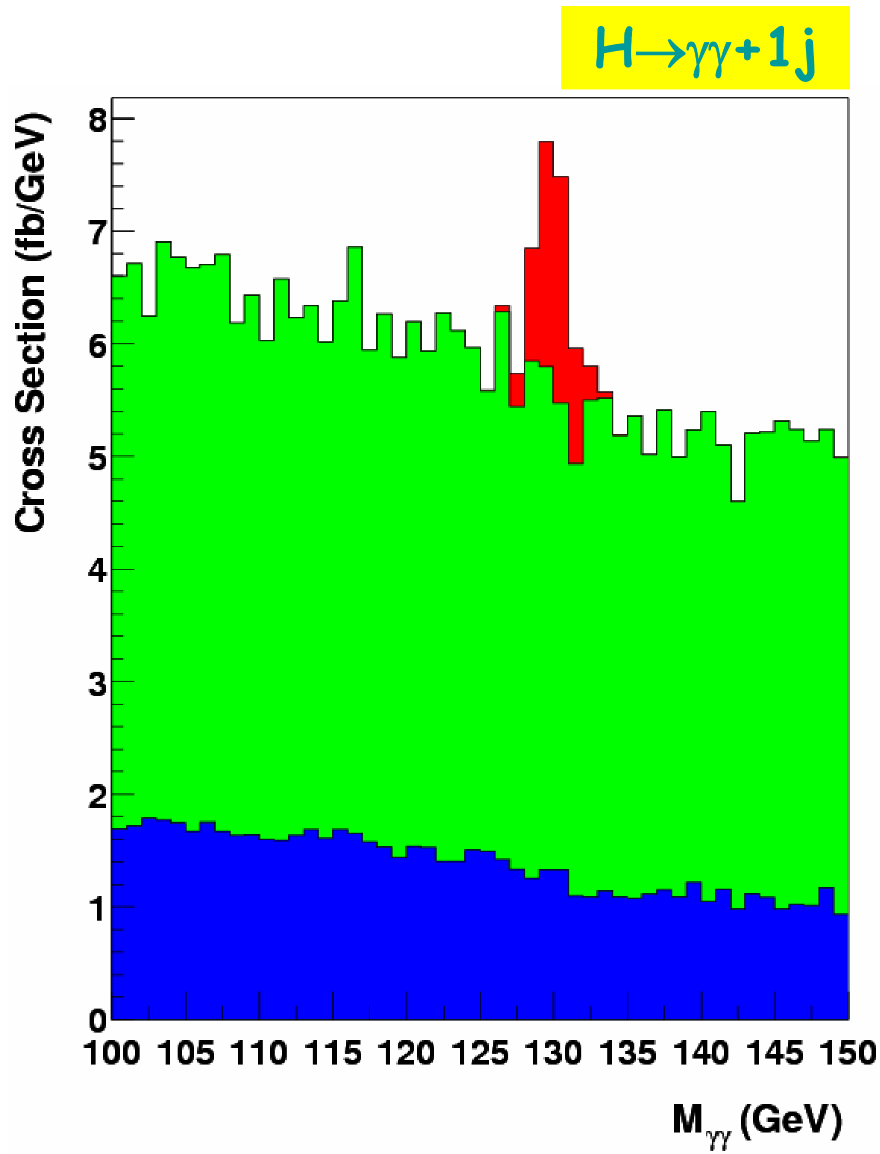

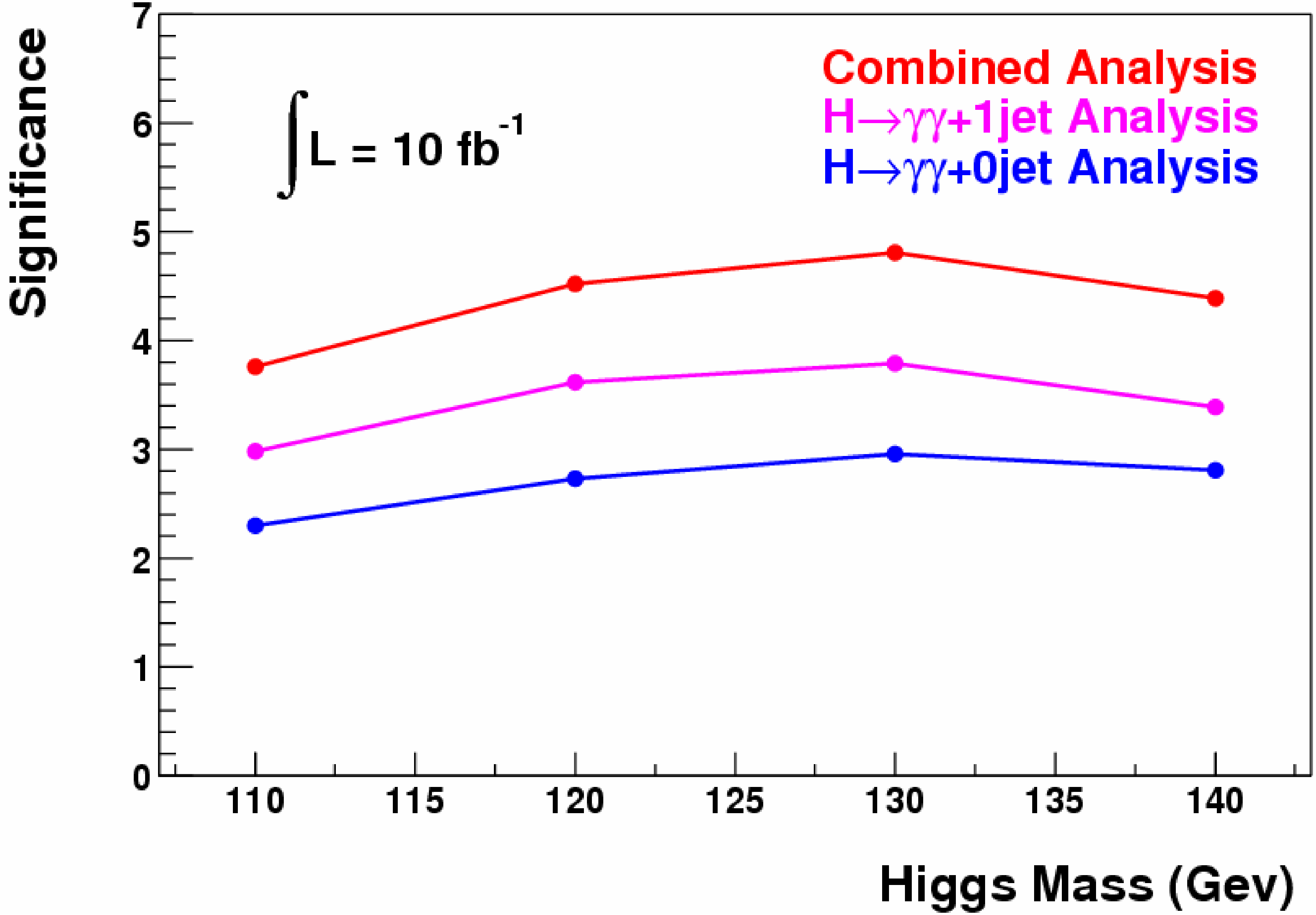

Significance
$\int L = 10\ fb^{-1}$
Combined Analysis
$H \rightarrow \gamma\gamma$+1jet Analysis
$H \rightarrow \gamma\gamma$+0jet Analysis
0
1
2
3
4
5
6
7
110
115
120
125
130
135
140
Higgs Mass (Gev)

Vertex Correction

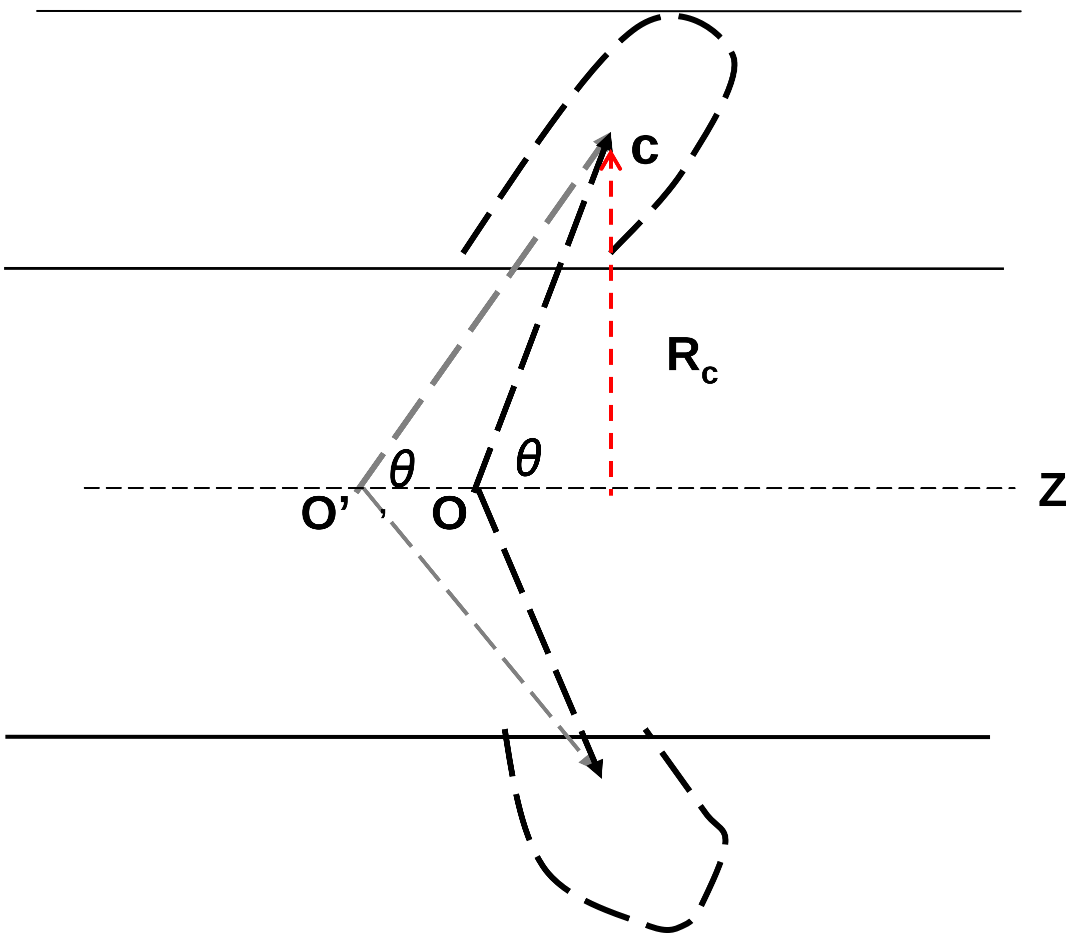

Z: Beam Axis
O: (0,0,0) of Atlas coord. system
O': Event Interaction Point
C: shower center in calorimeter
R_C: radius of shower center

We use the shower depth parameterization to calculate shower center

$$t = \frac{X}{X_0} \quad material \quad depth$$

$$t_{max} = \ln \frac{E_0}{E_c} - 1 \quad of \quad the \quad shower$$

$$E_c \approx \frac{560\ MeV}{Z}$$

- Application of vertex correction (correction of photon angles using position of vertex) improves Higgs mass resolution by 27%

MC@NLO M_H=130GeV DC1/7.0.2

Before Vertex Correction

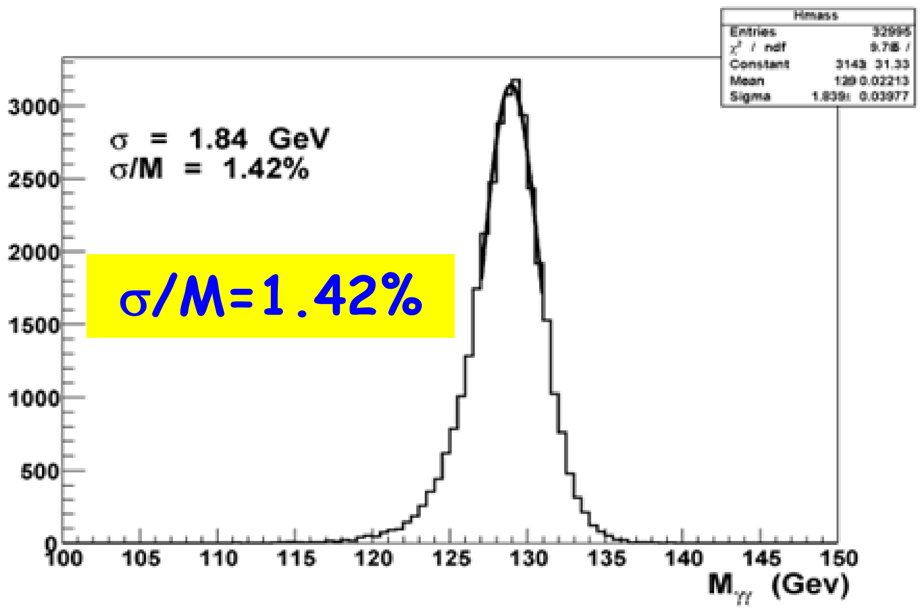

After Vertex Correction

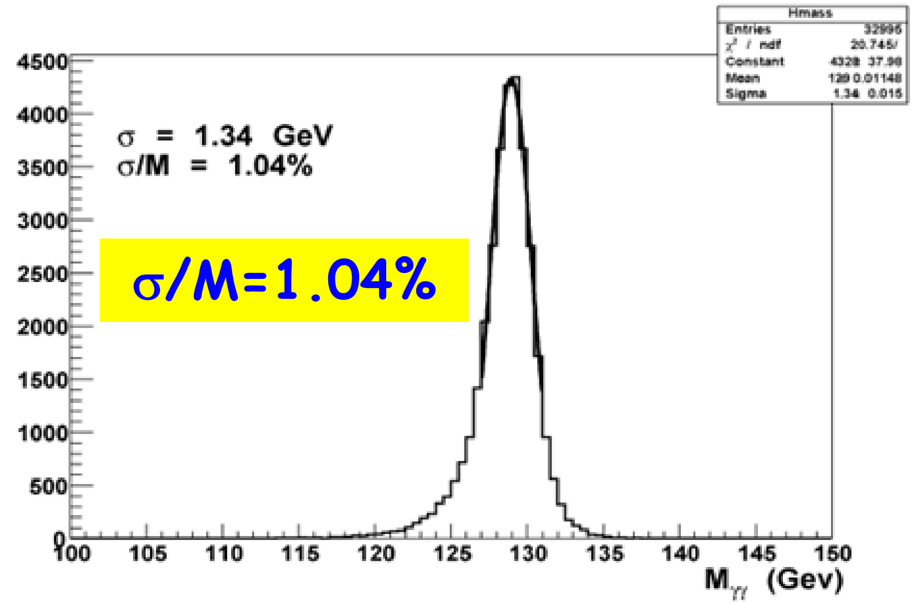

Gauge mediated SUSY breaking models

(SUSY breaking scale of messenger sector $)^2/M_m$

Messenger mass

M(gravitino) < 1 GeV

NLSP → gravitino + · ·

Table 20-16 Parameters of the four GMSB points considered in Section 20.3.

Point	Λ(TeV)	M_m(TeV)	N_5	$\tan\beta$	sgnμ	C_{grav}	
G1a	90	500	1	5.0	+	1.0	← short lifetime
G1b	90	500	1	5.0	+	10^3	← long lifetime
G2a	30	250	3	5.0	+	1.0	
G2b	30	250	3	5.0	+	5×10^3	

Table 20-17 Masses in GeV for the particles at the GMSB points in Table 20-16 from ISAJET 7.37 [20-15]. Only the gravitino mass depends on C_{grav}.

Particle	Point G1	Point G2	Particle	Point G1	Point G2	Particle	Point G1	Point G2	
$\tilde{g}$	747	713	$\tilde{u}_L$	986	672	$\tilde{e}_L$	326	204	
$\tilde{\chi}_1^{\pm}$	223	201	$\tilde{u}_R$	942	649	$\tilde{e}_R$	164	103	
$\tilde{\chi}_2^{\pm}$	469	346	$\tilde{d}_L$	989	676	$\tilde{\nu}_e$	317	189	
$\tilde{\chi}_1^0$	119	116	$\tilde{d}_R$	939	648	$\tilde{\tau}_1$	163	102	← NLSP
$\tilde{\chi}_2^0$	224	204	$\tilde{t}_1$	846	584	$\tilde{\tau}_2$	326	204	
$\tilde{\chi}_3^0$	451	305	$\tilde{t}_2$	962	684	$\tilde{\nu}_\tau$	316	189	
$\tilde{\chi}_4^0$	470	348	$\tilde{b}_1$	935	643	h	110	107	
			$\tilde{b}_2$	945	642	H	557	360	
						A	555	358	
						$H^{\pm}$	562	367	

GMSB G2b point

NLSP = $\tilde{\tau}_1$ and $c\tau \approx 1\,\mathrm{km}$

$\tilde{e}_R$ and $\tilde{\mu}_R$ are also long-lived

➔ stable heavy charged leptons

$\tilde{\chi}_i^0 \rightarrow \tilde{\ell}_R \ell$

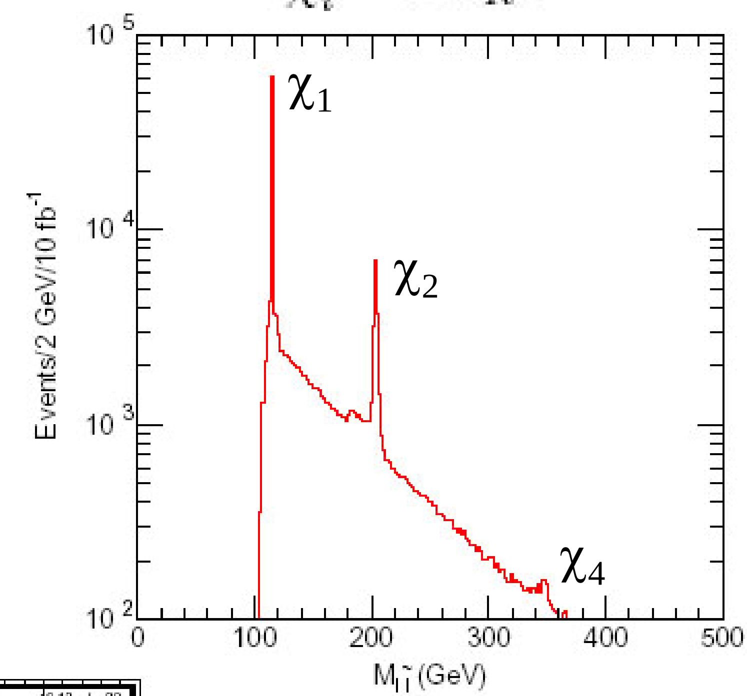

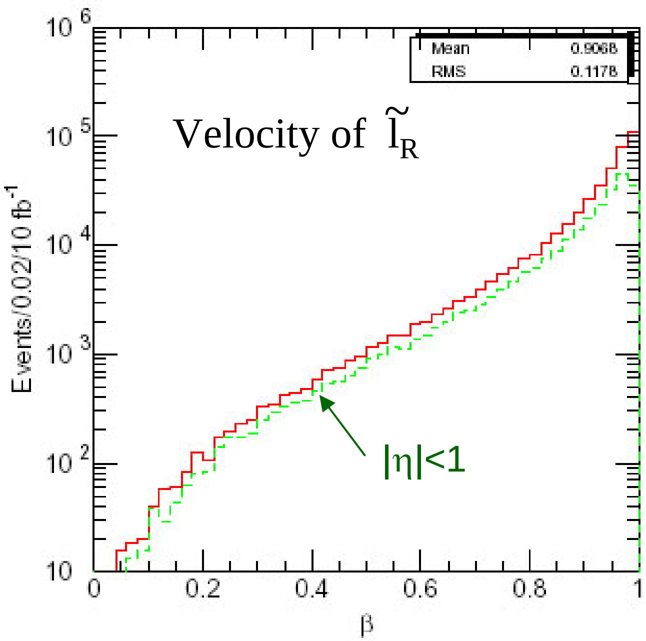

ATLAS MDT ➔ $\sigma_t \sim 1$ns

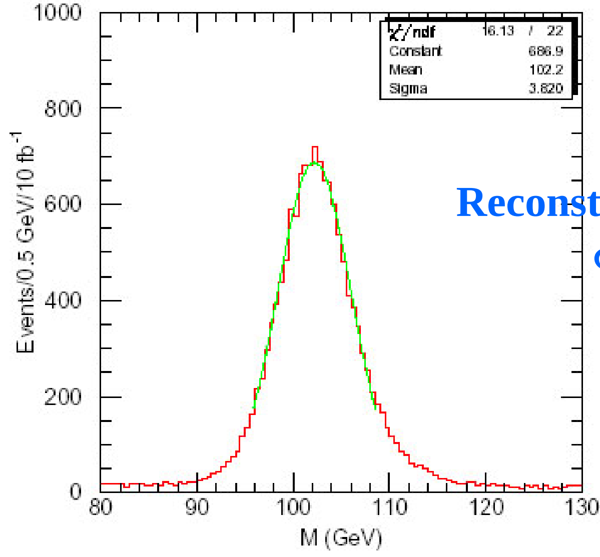

Reconstructed slepton mass

σ_M / M ~ 4%

→トリガーは大丈夫か？

A Possible Gauge Mediation Signal

$$\tilde{\chi}_1^0 \rightarrow \gamma \tilde{G}$$

cτ ~ O(1m)

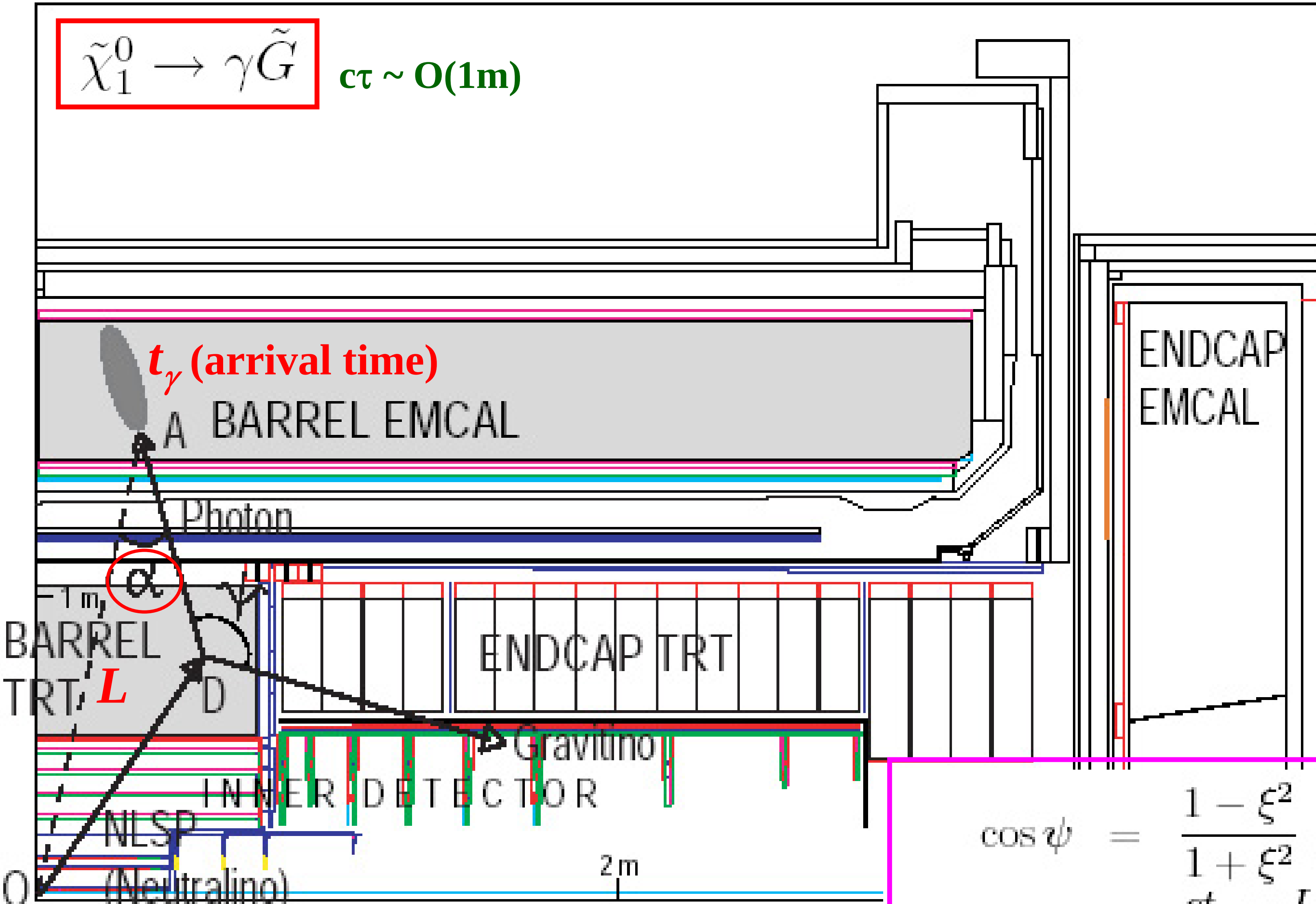

$$\cos\psi = \frac{1-\xi^2}{1+\xi^2},$$

$$\text{where}\quad \xi \equiv \frac{ct_\gamma - L\cos\alpha}{L\sin\alpha}$$

Gravitinoの方向が決まる

EM Calorimeter Performance

物理のベンチマーク･プロセス　H→$\gamma\gamma$、4$e^{\pm}$

検出器　… 4元運動量（E,**p**）or (t,**x**)を測定するのが良い。例：Kamiokande

ATLAS Liquid Argon カロリメーターは、これが出来る！

- エネルギー分解能　　$\sigma/E=10\%/\sqrt{E} \oplus 200(400)\mathrm{MeV}/E \oplus 0.7\%$
- 角度分解能　　**4-6 mrad/√E**（φ方向、Middle Layer(第2層)）
  50 mrad/√E（η方向、Strip+Middle Layer→Z vertexの測定）
- 時間分解能　　**100 ps** (1ns at 1GeV)
- 粒子識別　　$e^{\pm}$/jets, γ/π^0 > 3 at E_T=50GeV
- Linearity　　< 0.1%
- Dynamic range　　20MeV(MIP粒子μも検出可能) - 2TeV（余剰次元などの信号）

ϕ方向は？

本当か？

- ATLAS Liquid Argonカロリメーター
  - 鉛／液体アルゴンのサンプリング･カロリメーター（アコーディオン型）
  - Azimuthal角＝2π（クラック無し）、擬ラピディティー η<3.2 (FCAL <4.9)をカバー。
  - Liquid Argonは、intrinsicにrad-hard。
  - アコーディオン･ジオメトリー

Time resolution

4th ATLAS Physics Workshop
(Athens, May 2003)
LAr EM Calorimeter: Results from Beam Tests
F. Djama – CPPM Marseille

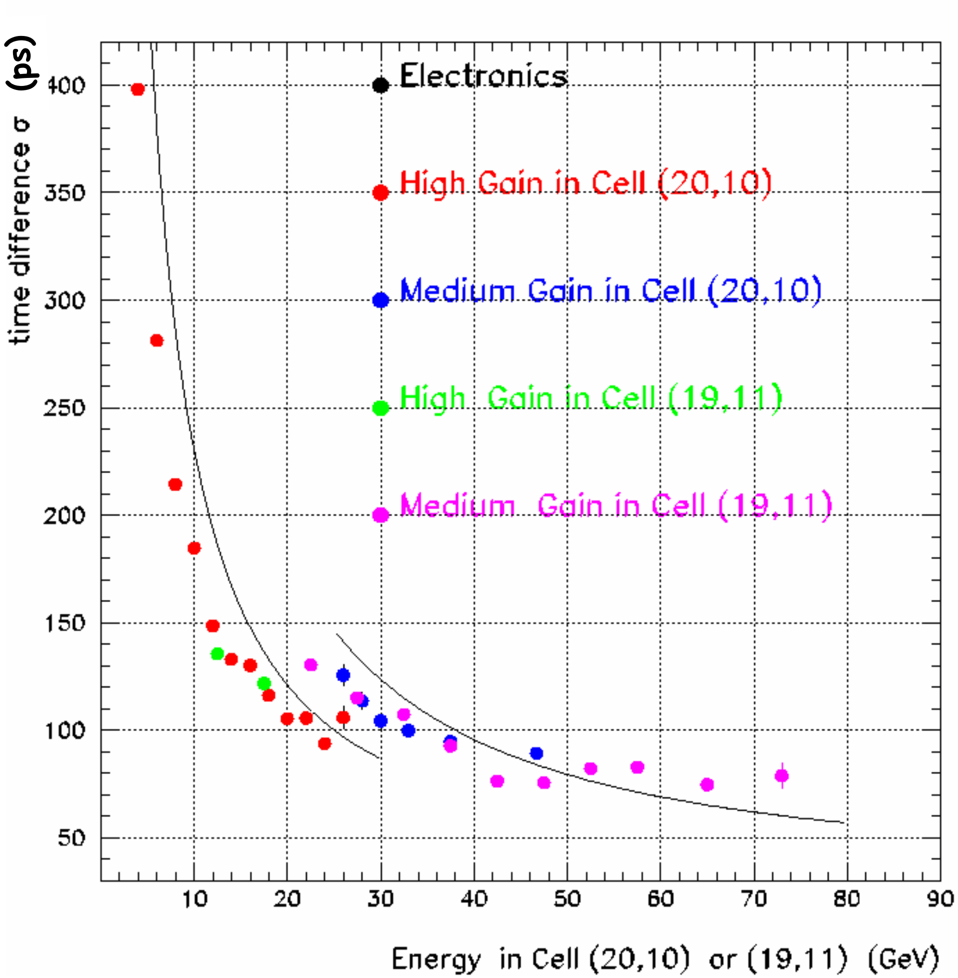

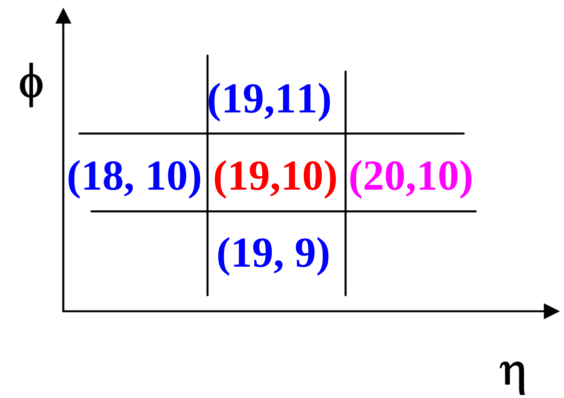

Resolution:
~70 ps @70GeV

A Possible Gauge Mediation Signal

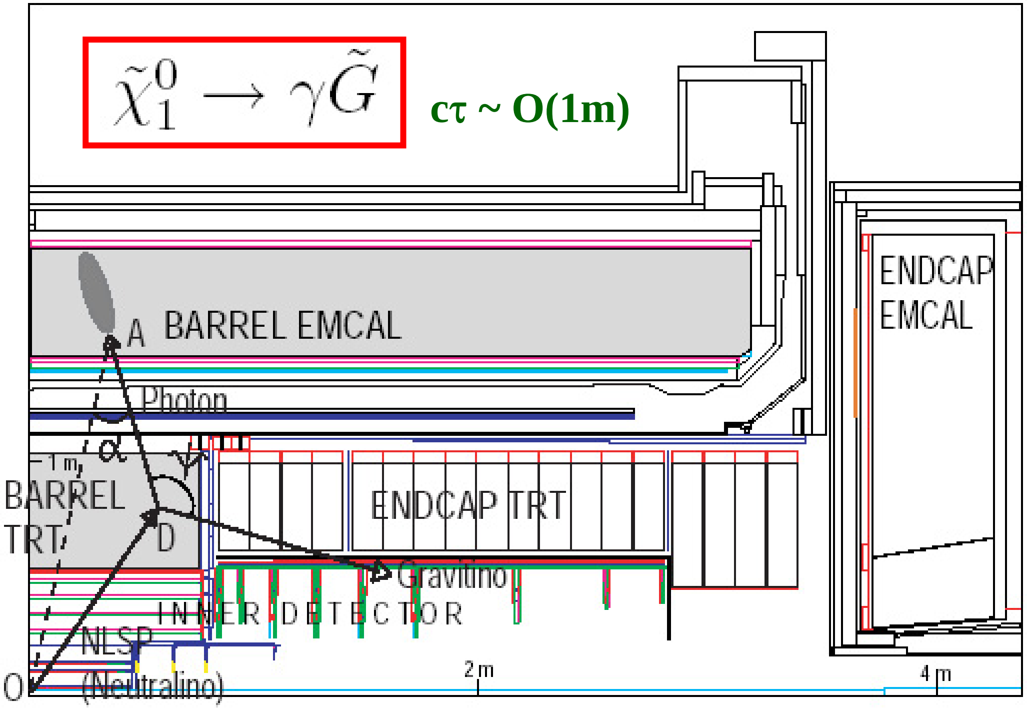

$$\tilde{\ell} \rightarrow \ell \tilde{\chi}_1^0 \rightarrow \ell \gamma \tilde{G}$$

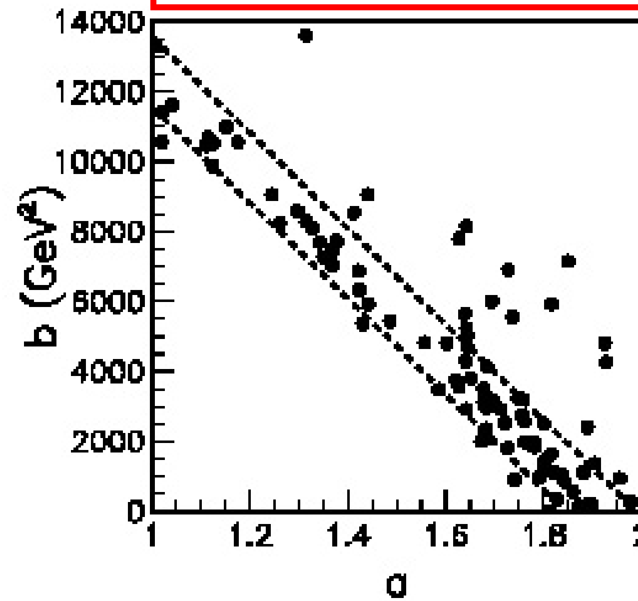

$$\begin{aligned} m_{\tilde{\ell}}^2 &= (p_\gamma + p_{\tilde{G}} + p_\ell)^2 \\ &= 2E_\gamma E_{\tilde{G}}(1-\cos\psi) + 2E_\ell E_{\tilde{G}}(1-\cos\theta_{\ell\tilde{G}}) \\ &+ 2E_\ell E_\gamma(1-\cos\theta_{\ell\gamma}) \\ &= \underbrace{\left(1 + \frac{E_\ell(1-\cos\theta_{\ell\tilde{G}})}{E_\gamma(1-\cos\psi)}\right)}_{a} m_{\tilde{\chi}_1^0}^2 + \underbrace{2E_\ell E_\gamma(1-\cos\theta_{\ell\gamma})}_{b} \end{aligned}$$

$$\begin{aligned} \cos\psi &= \frac{1-\xi^2}{1+\xi^2}, \\ \text{where} \quad \xi &\equiv \frac{ct_\gamma - L\cos\alpha}{L\sin\alpha} \end{aligned}$$

→ missing-E_T 不要

~100 lγ events ➔ σ_M/M (slepton, neutralino) ~ 3%

PRD69(2004)035003

今日の話の結論

アトラス検出器の性能をよく知り、その特徴を活かした解析を目指してください。

（CMSとの比較でATLASのほうが優れているものは？）

Motivationを持って、自分で調べてください。
（必要なら検出器の改良へ）

いきなりMC simulationに頼らずに、まず手で当たりをつける習慣を！